CERN-TH.4578/86
MAD/TH/86-26

SEARCH FOR NEW QUARKS SUGGESTED BY THE SUPERSTRING

V.D. Angelopoulos*), J. Ellis, H. Kowalski+), D.V. Nanopoulos‡),
N.D. Tracas and F. Zwirner&)

CERN - Geneva

ABSTRACT

We discuss the possible phenomenology of the additional charge (-1/3) colour triplet particles $D_{\frac{1}{2}}$ of spin $\frac{1}{2}$ and D_o, $\bar{D}_o^c$ of spin 0 which are contained in each matter generation if the superstring is compactified on a Calabi-Yau manifold. In the minimal model with no intermediate mass scales and supersymmetry breaking fed into the observable sector via a gaugino mass, either a spin-$\frac{1}{2}$ or a spin-0 D particle could be the lightest, and either could be as light as the present lower bound from e^+e^- experiments of about 20 GeV. The D particles could behave as leptoquarks coupling to quarks and leptons, in which case the single production process $ep \to D_o(\bar{D}_o^c)+X$ would occur, and $D_o(\bar{D}_o^c) \to \ell q$, $D_{\frac{1}{2}} \to \ell q\tilde{\chi}$ decays would dominate, where $\tilde{\chi}$ is the lightest supersymmetric particle. Alternatively, the D particles could behave as diquarks coupling to pairs of antiquarks, in which case the single production process $\overset{(-)}{p}p \to D_o(\bar{D}_o^c, \bar{D}_o, D_o^c)+X$ would occur, and $D_o(\bar{D}_o^c) \to \bar{q}\bar{q}$, $D_o^c(\bar{D}_o) \to qq$, $D_{\frac{1}{2}} \to \bar{q}\bar{q}\tilde{\chi}$ decays would dominate. We present cross-sections for $ep \to D_o(\bar{D}_o^c)+X$, $\overset{(-)}{p}p \to D_o(\bar{D}_o^c, D_o^c, \bar{D}_o)+X$, $e^+e^- \to D_o\bar{D}_o(D_o^c\bar{D}_o^c)$ and $D_{\frac{1}{2}}\bar{D}_{\frac{1}{2}}$, $\overset{(-)}{p}p \to D_o\bar{D}_o(D_o^c\bar{D}_o^c)$ and $D_{\frac{1}{2}}\bar{D}_{\frac{1}{2}}+X$. We calculate the experimental signals and estimate backgrounds for D production and decay in these processes. The decays $D_o(\bar{D}_o^c) \to \ell q$ and $D_{\frac{1}{2}} \to \ell q\tilde{\chi}$ or $\bar{q}\bar{q}\tilde{\chi}$ would be detectable in most of these reactions, but $D_o(\bar{D}_o^{c\frac{1}{2}}) \to \bar{q}\bar{q}$ decays may only be detectable in $e^+e^- \to D_o\bar{D}_o$ $(D_o^c\bar{D}_o^c)$ collisions.

---

*) Also at Dept. of Theoretical Physics, University of Oxford, Oxford, United Kingdom.
+) Permanent address: DESY, Hamburg, F.R. Germany.
‡) Permanent address: Dept. of Physics, University of Wisconsin, Madison USA.
&) Also at International School for Advanced Studies, Trieste and INFN, Padova, Italy. Address after 1 November 1986: Lawrence Berkeley Laboratory, University of California, Berkeley, USA.

CERN-TH.4578/86
MAD/TH/86-26
October 1986

1. - INTRODUCTION

The low-energy phenomenology of the superstring[1] depends on the compactification scheme which is adopted. An attractive proposal which avoids many theoretical and phenomenological pitfalls is that the six unseen dimensions are compactified on a Kähler manifold of SU(3) holonomy and zero torsion[2]. In this case the observable particles appear in generations containing 27 fields with the quantum numbers of the fundamental representation of E_6, plus possible split multiplets coming from $\underline{27}+\overline{\underline{27}}$ representations of E_6, and the four-dimensional observable gauge group is some rank 5 or 6 subgroup of E_6[3]. In some models this gauge group is broken by the Higgs mechanism, and the light particles do not include all the fields in a $\underline{27}$ of E_6. However, it is quite possible that some exotic matter particles survive down to low energies. Thus one can expect in many of the conceivable symmetry-breaking patterns to see additional matter particles and/or gauge interactions at low energies. Although they have not yet been worked out in detail, some orbifold compactifications[4] could offer similar phenomenological possibilities[5].

Constraints on additional neutral current effects at low energies have been discussed extensively[6),7], as well as possible signals of new gauge bosons at future colliders[8]. The possible phenomenology of colour-singlet superstring particles has also been explored[9]. This paper is concerned with the possible signatures of additional colour-triplet superstring particles. These have also been previously discussed[10], though the emphasis of previous studies has been somewhat different from that taken in this work.

We start with a pedagogical discussion of the particle content and of the possible interactions of the 27 fields in the fundamental representation of E_6. The $\underline{27}$ representation splits up under SO(10) to $\underline{16}+\underline{10}+\underline{1}$ and then under SU(5) to $(\underline{10}+\overline{\underline{5}}+\underline{1}) + (\underline{5}+\overline{\underline{5}}) + \underline{1}$. According to the conventional assignment, the usual quarks and leptons are members of the first $\underline{10}$ and $\overline{\underline{5}}$. The states of the additional 5 and $\overline{\underline{5}}$ can be identified with the usual Higgs doublets H and $\bar{H}$, and as new additional colour triplets D and D^c. There is also an additional SO(10) and SU(5) singlet called N, and an SU(5) [but not SO(10)] singlet called ν^c.

The decomposition of the $\underline{27}$ representation under the standard model subgroup $G_o \equiv SU(3)_C \times SU(2)_L \times U(1)_Y$ consists of the following left-handed multiplets:

$$Q \equiv \begin{pmatrix} u \\ d \end{pmatrix} \sim (3, 2, +1/6)\,, \quad u^c \sim (\bar{3}, 1, -2/3)\,, \quad e^c \sim (1, 1, +1)\,,$$

$$D \sim (3, 1, -1/3)\,, \quad H \equiv \begin{pmatrix} H^+ \\ H^o \end{pmatrix} \sim (1, 2, +1/2)\,; \tag{1.1}$$

$$d^c, D^c \sim (\bar{3}, 1, +1/3)\,, \quad L \equiv \begin{pmatrix} \nu \\ e \end{pmatrix}\,, \quad \bar{H} \equiv \begin{pmatrix} \bar{H}^o \\ \bar{H}^- \end{pmatrix} \sim (1, 2, -1/2),$$

$$N, \nu^c \sim (1, 1, 0)\,. \tag{1.2}$$

The first two numbers in brackets denote the dimensions of the $SU(3)_C$ and $SU(2)_L$ representations respectively, and the third one the $U_Y(1)$ hypercharge. The above states have, besides the usual gauge couplings, also generalized Yukawa interactions. The most general superpotential couplings allowed by the Hosotani[11] symmetry-breaking mechanism, which is the only one presently available for breaking E_6 down to an acceptable subgroup at the compactification scale, are[3]:

$$f = h_U Q u^c H + h_E L e^c \bar{H} \tag{1.3a}$$

$$+ h_\nu H L \nu^c + \lambda H \bar{H} N \tag{1.3b}$$

$$+ \lambda_\nu D d^c \nu^c + k D D^c N \tag{1.3c}$$

$$+ \lambda_L Q D^c L + h_D Q d^c \bar{H} \tag{1.3d}$$

$$+ \lambda_e D e^c u^c + \lambda_Q D Q Q + \lambda_c D^c u^c d^c. \tag{1.3e}$$

In a conventional GUT, the couplings h_u, h_E, h_ν, λ ... would be related by Clebsch-Gordan coefficients of order unity, and therefore the new states D and D^c would need to be very heavy in order to avoid rapid proton decay[12]. The new feature of the string compactification scenario is that not only is the GUT gauge group broken by the Hosotani[11] mechanism, but also the Clebsch-Gordan relations

between Yukawa couplings are broken[3]. This leads to the phenomenologically interesting possibility that the new colour triplets D and D^c could be light and behave either as leptoquarks or as diquarks.

The D and D^c particles acquire their mass through the vacuum expectation value of the N field. The fermionic members of the D/D^c supermultiplets will combine into Dirac fermions of mass $m_D = k\langle 0|N|0\rangle$, denoted here by $D_{\frac{1}{2}}$. The masses of their scalar partners D_o, D_o^c receive additional contributions from soft supersymmetry-breaking terms which are of the same order as conventional Higgs or squark masses, and hence are expected to be $O(m_W$ to 1 TeV). It is possible that $\langle 0|N|0\rangle$ is very large, but in that case the $H\bar{H}N$ coupling (1.3b) would need to be very small in order for $\langle 0|H,\bar{H}|0\rangle$ to be $O(m_W)$ as required. It is therefore interesting to study the case that $\langle 0|N|0\rangle$ is not very much larger than m_W, where one expects both the $D_{\frac{1}{2}}$ fermions and the D_o, D_o^c bosons to weigh $\lesssim O(1)$ TeV and hence be accessible to experiment. A priori, one could have mixing between d^c and D^c and between leptons and Higgses $\bar{H}$. We discuss this problem carefully in Section 2 and argue that in the context of a minimal model there are no rotations between these sectors to be considered [for an alternative point of view, see Ref. 10)].

The non-observation of supersymmetric particles and the absence of additional neutral current effects constrain the parameters of superstring models and hence the possible masses of the $D_{\frac{1}{2}}$ and D_o, D_o^c particles. We analyze these constraints in Section 2, working in the context of a minimal rank-5 low-energy model[6], where the dominant source of supersymmetry breaking in the observable sector is a gaugino mass term. We also incorporate more model-dependent constraints which follow from dynamical calculations of radiative electroweak breaking in this special theoretical framework. We find that some of the $D_{\frac{1}{2}}$ and D_o, D_o^c particles could be as light as the present bounds on new particles in e^+e^- collisions: $m \gtrsim 20$ GeV. The D particles could be produced by single or pair production mechanisms. Single production could proceed through quark-quark annihilation in hadron-hadron collisions or quark-lepton annihilation in ep collisions through the diquark and leptoquark couplings of Eq. (1.3). The two processes cannot happen simultaneously, because otherwise rapid proton decay could be mediated by D_o exchange. The couplings of the D particles which influence their possible production mechanisms and decay signatures are discussed in Section 3. The cross-sections for these two single production mechanisms are calculated and compared with conventional backgrounds. We find that the process

$ep \to (D_o/D_o^c \to q\ell) + X$ could be observable at HERA if the D_o mass is below ~ 250 GeV. The diquark annihilation process which could take place at the hadron-hadron colliders, $\overset{(-)}{p}p \to D_o/D_o^c \to \bar{q}\bar{q}/qq + X$ would, however, be overwhelmed by the conventional QCD jet-jet background. However, the pair-production process could be a source of observable D particles at hadron-hadron colliders. In Section 4 we calculate cross-sections for the possible pair-production mechanisms $hh \to D_o\bar{D}_o$ $(D_o^c\bar{D}_o^c) + X$ and $D_{\frac{1}{2}}\bar{D}_{\frac{1}{2}} + X$ which proceed through the conventional strong interactions, and explore the possible event signatures. Since the gauge couplings of D particles are the same as those of usual quarks, these cross-sections are comparable to those for conventional squarks or t quarks respectively. The decays $D_o/\bar{D}_o^c \to q+\nu$, $\bar{D}_o/D_o^c \to \bar{q}+\nu$, $D_{\frac{1}{2}} \to q+\nu+\tilde{\chi}$ and $D_{\frac{1}{2}} \to \bar{q}+\bar{q}+\tilde{\chi}$, where $\tilde{\chi}$ denotes the lightest supersymmetric particle, have missing energy signatures analogous to those expected for conventional squarks and gluinos[13]. The present UA1 missing energy search[14] may be able to exclude D_o or $D_{\frac{1}{2}}$ weighing up to O(60) GeV, but this needs to be investigated by the experimentalists themselves. Any such limit could be improved by future experiments using ACOL at CERN, or the Tevatron Collider. The decays $D_{\frac{1}{2}} \to q+\ell+\tilde{\chi}$ give experimental signatures with leptons, jets and missing energy which could have shown up in the UA1 dimuon sample[15] or in their top search, and again present data might have sensitivity for $m_{D_{\frac{1}{2}}} \lesssim 60$ GeV. The decays $D_o(\bar{D}_o^c) \to \bar{q}+\bar{q}$ and $\bar{D}_o(D_o^c) \to q+q$ would give four-jet final states which would be drowned by the QCD four-jet background, but the decays $D_o/\bar{D}_o^c \to q\ell$ $(\bar{D}_o/D_o^c \to \bar{q}\bar{\ell})$ would give dilepton + dijet signatures which should be easier to detect, and could show up in the UA1 dimuon sample[15]. A useful limit on them could perhaps be obtained with present data.

Finally, Section 5 presents some conclusions and proposes some possible directions for future experiments which could search for D particles.

2. - CONSTRAINTS ON THE (D_o, D_o^c) AND $D_{\frac{1}{2}}$ MASSES

Here we discuss in detail the mass matrices for the exotic quarks $D_{\frac{1}{2}}$ and squarks D_o, D_o^c in the realistic case of $n_G = 3$ generations. Where it is necessary to be specific, we will work in the framework of the minimal rank-5 gauge group[6]

which can be provided by Hosotani symmetry breaking. However, the following analysis could be extended to any similar model with light exotic quarks and squarks.

First we discuss the possibility mentioned in Section 1 of mixings between the fields d^c and D^c, L and $\bar{H}$, ν^c and N, which are seen from Eq. (1.2) to have identical $SU(3)_c \times SU(2)_L \times U(1)_Y$ quantum numbers. If the low-energy group commutes with $SU(2)_N$, which is the case for the minimal model, we may without loss of generality identify L with the standard lepton doublet, in which case lepton number conservation requires $\langle 0|\tilde{\nu}|0\rangle = 0$. In order to identify the mass eigenstates corresponding to the ordinary charge -1/3 quarks and charged leptons, one must examine the corresponding mass matrices, which take the forms

$$(d,D)\, M_{1/3} \begin{pmatrix} d^c \\ D^c \end{pmatrix} \quad : \quad M_{1/3} = \begin{pmatrix} h_D \langle 0|\bar{H}^0|0\rangle & 0 \\ \lambda_\nu \langle 0|\tilde{\nu}^c|0\rangle & k\langle 0|N|0\rangle \end{pmatrix} \tag{2.1}$$

and

$$(e^c,\, H^+)\, M_1 \begin{pmatrix} e \\ \bar{H}^- \end{pmatrix} : \quad M_1 = \begin{pmatrix} h_E \langle 0|\bar{H}^0|0\rangle & 0 \\ h_\nu \langle 0|\tilde{\nu}^c|0\rangle & \lambda\langle 0|N|0\rangle \end{pmatrix}. \tag{2.2}$$

The physical masses are given by the eigenvalues of the matrices $M^+_{1/3}M_{1/3}$ and $M_1^+M_1$ respectively. We assume for simplicity real Yukawa coupling constants and vacuum expectation values (vevs). Note that, in order to avoid unacceptable zero mass eigenvalues in (2.1) and (2.2), it must be that $\langle 0|N|0\rangle \neq 0$. On the other hand, the possibilities that $\lambda^D\langle 0|\tilde{\nu}^c|0\rangle$, $\lambda^L\langle 0|\tilde{\nu}^c|0\rangle \neq 0$ have potential phenomenological problems with flavour-changing neutral currents and the physical values of m_d, m_e [17]. Thus we will assume in the rest of this paper that $\langle 0|\tilde{\nu}^c|0\rangle = 0$, which implies $\langle 0|\bar{H}^\circ|0\rangle \neq 0$ to avoid zero eigenvalues in (2.1) and (2.2). It must also be that $\langle 0|H^\circ|0\rangle \neq 0$ to give masses to the quarks of charge $\pm 2/3$. We are then led to a situation where we can identify (d,d^c) with the ordinary quarks (of mass $h_D \langle 0|\bar{H}^\circ|0\rangle$) and (D,D^c) with the new exotic quarks (of mass $k\langle 0|N|0\rangle$), and there is no mixing between the two sectors. Similarly, we will identify (e,e^c) with the ordinary leptons, and $(H^+, \bar{H}^-)$ with the charged Higgs fields.

In the case of a three-generation model, the fields which can acquire non-

vanishing VEVs are H_a°, $\bar{H}_a^\circ$ and N_a, where a = 1,2,3 is a generation index. However, it is always possible[18] to redefine those fields, via independent rotations in generation space, in such a way that $\langle 0|H_a^\circ|0\rangle = \langle 0|\bar{H}_a^\circ|0\rangle = \langle 0|N_a|0\rangle = 0$ for a = 1,2 and the only non-vanishing VEVs are:

$$\langle 0|H_3^\circ|0\rangle \equiv U \quad , \quad \langle 0|\bar{H}_3^\circ|0\rangle \equiv \bar{U} \quad , \quad \langle 0|N|0\rangle \equiv x \ . \tag{2.3}$$

In this new basis, the part of the superpotential contributing to the $D_{\frac{1}{2}}$ masses is simply:

$$f^{\text{mass}}_{D_{1/2}} = k_{ab3}\, D_a\, D^c_b N_3 \ . \tag{2.4}$$

We have not used, up to now, the freedom of redefining the fields D_a and D^c_a by independent rotations in generation space. We can therefore move to a convenient basis where the following relations hold:

$$k_{ab3} = 0 \qquad \text{for} \qquad a \neq b \ . \tag{2.5}$$

Assuming, without loss of generality, that x > 0, the two-component spinors of each generation contained in the chiral superfields D_a, D^c_a will then combine to form three Dirac spinors $D_{\frac{1}{2}a}$ of masses

$$m_{D_a} = |k_{aa3}| \cdot x \qquad (a = 1,2,3) \tag{2.6}$$

The mass matrix involving the scalar components of D_a and D^c_a has a slightly more complicated structure. Even in the convenient basis we chose above, one has in general a real symmetric 6×6 matrix, with non-trivial intergenerational mixing. The matrix elements are

$$M_{D_1\bar{D}_1} = \tilde{m}^2_{D_{11}} + m^2_{D_1} + G^2(D) \ , \quad M_{\bar{D}^c_1 D^c_1} = \tilde{m}^2_{D^c_{11}} + m^2_{D_1} + G^2(D^c) \ ,$$

$$M_{D_2\bar{D}_2} = \tilde{m}^2_{D_{22}} + m^2_{D_2} + G^2(D) \ , \quad M_{\bar{D}^c_2 D^c_2} = \tilde{m}^2_{D^c_{22}} + m^2_{D_2} + G^2(D^c) \ ,$$

$$M_{D_3\bar{D}_3} = \tilde{m}^2_{D_{33}} + m^2_{D_3} + G^2(D) \ , \quad M_{\bar{D}^c_3 D^c_3} = \tilde{m}^2_{D^c_{33}} + m^2_{D_3} + G^2(D^c) \ ,$$

$$M_{D_1 D_1^c} = \eta^K_{113} x + \sum_{1}^{3}{}_c \lambda_{33c} k_{11c} v\bar{v} \;, \quad M_{D_1 \bar{D}_2} = \tilde{m}^2_{D_{12}} \;,$$

$$M_{D_1 D_2^c} = \eta^U_{123} x + \sum_{1}^{2}{}_c \lambda_{33c} k_{12c} v\bar{v} \;, \quad M_{D_1 \bar{D}_3} = \tilde{m}^2_{D_{13}} \;,$$

$$M_{D_1 D_3^c} = \eta^U_{133} x + \sum_{1}^{2}{}_c \lambda_{33c} k_{13c} v\bar{v} \;,$$

$$M_{\bar{D}_1^c \bar{D}_2} = \eta^U_{213} x + \sum_{1}^{2}{}_c \lambda_{33c} k_{21c} v\bar{v} \;, \quad M_{\bar{D}_1^c D_2^c} = \tilde{m}^2_{D^c_{12}} \;, \quad M_{\bar{D}_1^c D_3^c} = \tilde{m}^2_{D^c_{13}} \;,$$

$$M_{\bar{D}_1^c \bar{D}_3} = \eta^U_{313} x + \sum_{1}^{2}{}_c \lambda_{33c} k_{31c} v\bar{v} \;,$$

$$M_{D_2 D_2^c} = \eta^U_{223} x + \sum_{1}^{3}{}_c \lambda_{33c} k_{22c} v\bar{v} \;, \quad M_{D_2 D_3^c} = \eta^U_{233} x + \sum_{1}^{2}{}_c \lambda_{33c} k_{23c} v\bar{v} \;,$$

$$M_{D_2 \bar{D}_3} = \tilde{m}^2_{D_{23}} \;,$$

$$M_{\bar{D}_2^c \bar{D}_3} = \eta^U_{323} x + \sum_{1}^{2}{}_c \lambda_{33c} k_{32c} v\bar{v} \;, \quad M_{\bar{D}_2^c D_3^c} = \tilde{m}^2_{D^c_{23}} \;,$$

$$M_{D_3 D_3^c} = \eta^U_{333} x + \sum_{1}^{3}{}_c \lambda_{33c} k_{33c} v\bar{v} \;. \tag{2.7}$$

Symbols appearing in the above formula correspond to the following general expressions for the superpotential and the soft supersymmetry-breaking part of the scalar potential:

$$f = \lambda_{abc} H_a \bar{H}_b N_c + k_{abc} D_a D^c_b N_c + \dots \;, \tag{2.8}$$

$$V_{soft} = \tilde{m}^2_{D_{ab}} D^*_a D_b + \tilde{m}^2_{D^c_{ab}} D^{c*}_a D^c_b + \dots$$
$$+ \eta^K_{abc} \left(D_a D^c_b N_c + \text{h.c.} \right) + \dots \tag{2.9}$$

where the dots represent terms which do not contribute to (2.7), m_{D_a} are the fermion masses given by Eq. (2.6) and a,b,c = 1,2,3. Moreover, $G^2(D)$ and $G^2(D^c)$ are the generation-independent D-term contributions to the scalar masses:

$$G^2(D) = \frac{5}{9} \frac{m_W^2 \tan^2\theta_W}{1 + (\bar{v}/v)^2} \left[1 + \left(\frac{\bar{v}}{v} \right)^2 - 2 \left(\frac{x}{v} \right)^2 \right] \;, \tag{2.10}$$

$$G^2(D^c) = \frac{5}{9}\,\frac{m_w^2 \tan^2\theta_w}{1+(\bar{v}/v)^2}\left[1-\frac{1}{2}\left(\frac{\bar{v}}{v}\right)^2-\frac{1}{2}\left(\frac{x}{v}\right)^2\right] \qquad (2.11)$$

To bring the discussion to a reasonable degree of simplicity, some short-cuts are necessary. Our first simplification is to assume that the only Yukawa couplings contributing significantly to the renormalization group equations (RGE) for the soft supersymmetry-breaking parameters are those diagonal in generation space (λ_{aaa}, k_{aaa}, ...). In this case, the soft supersymmetry-breaking part of the scalar potential assumes the simplified form:

$$V_{soft} = \tilde{m}^2_{D_a}\,|D_a|^2 + \tilde{m}^2_{D^c_a}\,|D^c_a|^2 + \ldots$$

$$+ \; k_{abc}\,A^{k}_{abc}\,(D_a D^c_b N_c + h.c.) + \ldots \qquad (2.12)$$

Moreover, the mass matrix (2.7) for D_o squarks becomes block-diagonal in generation space, with each 2×2 block given by

$$\mathcal{M}^2_{o_a} = \begin{pmatrix} \tilde{m}^2_{D_a} + m^2_{D_a} + G^2(D) & m_{D_a} A^{k}_{aa3} + \lambda_{333} k_{aa3} v\bar{v} \\ m_{D_a} A^{k}_{aa3} + \lambda_{333} k_{aa3} v\bar{v} & \tilde{m}^2_{D^c_a} + m^2_{D_a} + G^2(D^c) \end{pmatrix} \qquad (2.13)$$

Let us examine now the phenomenological constraints on the quantities appearing in Eqs. (2.6) and (2.13). These constraints are derived under the plausible assumption that the main source of supersymmetry breaking in the observable sector is a universal gaugino mass $m_{\frac{1}{2}}$ [19], assigned at the grand unification scale M_X, which in turn generates all the other SUSY-breaking parameters via radiative corrections, taken into account by the renormalization group equations.

Of the three VEVs v, $\bar{v}$ and x, only two combinations are independent since the constraint

$$m_W = \frac{e}{\sin\theta_W}\sqrt{\frac{v^2+\bar{v}^2}{2}} \simeq 82\ \text{GeV}$$

must be satisfied, where e is the running electric charge evaluated at $Q^2 \sim m_W^2$:

it is then convenient to have as independent parameters x/v and $\bar{v}/v$.

As other parameters appearing in (2.6) and (2.13), it is convenient to take $m_{\frac{1}{2}}$, $(\tilde{m}_{D_a}/m_{\frac{1}{2}})^2$, $(\tilde{m}_{D_a^c}/m_{\frac{1}{2}})^2$, $A^k_{aa3}/m_{\frac{1}{2}}$, λ_{333} and k_{aa3}. To simplify the discussion further, we shall assume that the only non-negligible Yukawa couplings contributing to the RGEs are indeed $\lambda_{333} \equiv \lambda$, $k_{333} \equiv k$ and $h_{\nu_{333}} \equiv h$ (where h provides the top quark mass), so that the RGEs can be written down in the simplified form used in Ref. 6). In this case, indicative ranges of variation for the different parameters are presented in Table 1. The lower limits on x/v and $m_{\frac{1}{2}}$ are derived from the present limits on sparticle masses and on the mass of a second neutral gauge boson. The corresponding upper limits resemble a form of naturalness constraint, and are more subjective. The ranges of variation of $\bar{v}/v$, λ_{333} and k_{333} are obtained from a detailed dynamical study of the effective scalar potential at low energy, solving numerically the RGEs for the soft SUSY-breaking parameters. The ranges of variation of $(\tilde{m}_{D_3}/m_{\frac{1}{2}})^2$, $(\tilde{m}_{D_3^c}/m_{\frac{1}{2}})^2$ and $A^k_{333}/m_{\frac{1}{2}}$ correspond to the solutions of the RGEs for allowed values of λ_{333}, k_{333} and of the top mass. The upper limits (in absolute value) correspond to small values of k_{333}, and vice versa*). The Yukawa coupling k_{333} must be greater than ~ 0.25 to generate the desired hierarchy $x/v \gtrsim 2.8$, and cannot be larger than ~ 0.55 if one wants to avoid charge- breaking minima. The other couplings k_{113} and k_{223} are assumed to be smaller than k_{333}, and there are no lower limits on them apart from the experimental limits on m_{D_a}.

Let us see now what are the indications on the $D_{\frac{1}{2}}$ and D_0 masses coming from explicit model calculations. To begin with, let us consider the $D_{\frac{1}{2}}$ masses, given by Eq. (2.6), which in terms of the parameters of Table 1 reads:

$$m_{D_a} = k_{aa3}\, x = k_{aa3}\left(\frac{x}{v}\right)\left\{2\sqrt{2}\, G_F\left[1+(\bar{v}/v)^2\right]\right\}^{-1/2} \qquad (2.14)$$

where $G_F = 1.166 \times 10^{-5}$ GeV^{-2} is the Fermi constant. Using the limits of Table 1, one finds $m_{D_3} \gtrsim 105$ GeV, while for a = 1,2 the lower limit on m_{D_a} is the experimental one:

$$m_{D_a} \gtrsim 20 \text{ GeV} \quad (a=1,2) \qquad (2.15)$$

---

*) For a = 1,2 we expect the corresponding quantities to be close to these limits, according to our assumption that $k_{113,223} \ll k_{333}$.

An indicative upper limit on the $D_{\frac{1}{2}}$ masses comes from the naturalness constraint, which forbids very large values of x/v, since they would require a fine tuning of the parameters in the scalar potential which would be unstable under radiative corrections[6]. Using the values of Table 1, one finds:

$$m_{D_1}, m_{D_2} < m_{D_3} \lesssim 1\ \text{TeV} \tag{2.16}$$

In summary, model calculations suggest for the $D_{\frac{1}{2}}$ quarks masses ranging from 20 GeV to 1 TeV. Although the scale of $D_{\frac{1}{2}}$ masses is generally the same as the scale of the extra Z' boson, since both are related to the breaking of the extra $U(1)_E$ gauge factor, some $D_{\frac{1}{2}}$ particles may be considerably lighter than the Z' if they have small Yukawa couplings to the N field which acquires a VEV.

Let us comment now on the structure of the D_o mass matrices, Eq. (2.13). First of all, note that, for the range of parameters given in Table 1, always $m_{D_a} A^k_{aa3} >> \lambda_{333} k_{aa3} v\bar{v}$, so that we can neglect this last contribution to the off-diagonal entry. Note also that, for large values of x/v, the D-term contributions of Eqs. (2.10) and (2.11) become negative and big. On the other hand, the positive contributions $\tilde{m}^2_{D_a}$ and $\tilde{m}^2_{D^c_a}$ are proportional to $m^2_{\frac{1}{2}}$. This suggests that light D_o masses can be obtained for relatively high values of (x/v) and relatively small values of $m_{\frac{1}{2}}$. However, detailed model calculations[6] exhibit a strong correlation between x/v and $m_{\frac{1}{2}}$; in particular, to avoid $(\text{mass})^2$ for the charged "unHiggses" $(H^+_a, \bar{H}^-_a)$, $(a = 1,2)$, which are too small or negative, a relation of the type $m_{\frac{1}{2}} > K_{cr}(x/v)$ must be satisfied, with K_{cr} slightly dependent on the other parameters, and generically in the range $K_{cr} \simeq 55 \div 65$ GeV. Even taking into account this last constraint, together with the correlation between $\tilde{m}^2_{D_a}$, $\tilde{m}^2_{D^c_a}$ and A^k_{aa3}, one finds the following results:

1) Calling D^1_{oa} and D^2_{oa} the two eigenvalues of the mass matrix (2.13), with masses $m_{D^1_{oa}} < m_{D^2_{oa}}$, the following two hierarchies are both possible:

$$m_{D_a} < m_{D^1_{oa}} < m_{D^2_{oa}} \tag{2.17a}$$

$$m_{D^1_{oa}} < m_{D_a} < m_{D^2_{oa}} \tag{2.17b}$$

2) Under our set of assumptions, masses of the D^1_{o3} ($D^1_{o1,2}$) squarks as low as 100 GeV (170 GeV) are allowed. These lower limits come from the study of the "unHiggs" mass spectrum, and have been derived under some model-dependent assumptions[6]. Relaxing these assumptions, they can be significantly lowered and could be as light as 20 GeV. On the other hand, the addition of a common scalar mass to the primordial soft SUSY-breaking terms would generally lead to higher D_{oa} masses, favouring the case of Eq. (2.17a) with respect to the one of Eq. (2.17b).

3) When the lowest possible values for the D^1_{oa} masses are attained, the mass eigenstate D^1_{oa} is always an admixture, with contributions of almost equal magnitude, of the interaction eigenstates D_a and $\overline{D^c_a}$.

This is essentially all the information on $D_{\frac{1}{2}}$, D_o masses that one is able to extract from model calculations. Despite all the constraints on the different parameters, there is still a large freedom for the resulting spectrum of $D_{\frac{1}{2}}$, D_o masses, which is not significantly bounded from below, thus motivating the phenomenological analysis of the following sections.

3. - SINGLE D PRODUCTION AND DECAY

3.1 D Couplings

As was mentioned in the Introduction, the D, D^c supermultiplets may couple directly to ordinary quarks and leptons through the following superpotential terms:

$$f \ni \lambda_Q D Q Q + \lambda_c D^c u^c d^c \qquad (3.1a)$$

$$+ \lambda_L D^c L Q + \lambda_e D u^c e^c \qquad (3.1b)$$

$$+ \lambda_\nu D d^c \nu^c \qquad (3.1c)$$

No other couplings are allowed by invariance under the E_6 Cartan subalgebra, which is maintained by the Hosotani gauge symmetry-breaking mechanism. In order to avoid rapid proton decay, the first row of couplings (3.1a) cannot be present

simultaneously with the second (3.1b) and third (3.1c) rows of possible terms in f. Topological zeroes and/or discrete symmetries could in principle forbid the disallowed combinations of couplings, though no explicit example has yet been exhibited. Dirac neutrino masses can be made to vanish naturally only if the couplings (λ_L, λ_e) of (3.1b) are not present simultaneously with the coupling λ_ν of (3.1c), and the same remarks about topological zeroes and/or discrete symmetries apply. We will take the sets (3.1a), (3.1b) and (3.1c) as alternative cases to study.

3.2 Couplings to Quarks

As discussed earlier, in the class of models we consider, no mixing of the D particles with conventional charge -1/3 quarks is possible. Single production of the scalar D is possible in hadron-hadron collisions via $\bar{q}+\bar{q} \to D_o$ $(q+q \to D_o^c)$, followed by $D_o \to \bar{q}+\bar{q}$ $(D_o^c \to q+q)$. The squared amplitudes $|M|^2$ for the decays of D_o and D_o^c to quark pairs are given by

$$|\mathcal{M}_{D_o}|^2 = 24 \lambda_q^2 m_{D_o}^2 \quad , \quad |\mathcal{M}_{D_o^c}|^2 = 6 \lambda_e^2 m_{D_o^c}^2 \tag{3.2}$$

and we have no idea what the ratio of the couplings λ_Q and λ_c might be. The differential cross-section for the process $h+h \to (D_o \to qq)+X$ is given by

$$d^2\sigma = (1/48\pi)\hat{s} \left\{u(x_1)d(x_2) + u(x_2)d(x_1) + \dots\right\} dx_1 dx_2 \, \delta(sx_1x_2 - \hat{s}) \cdot$$

$$\left\{ \frac{\lambda_q^4 (64/9)}{((\hat{s}-m_{D_o}^2)^2 + \Gamma_{D_o}^2 m_{D_o}^2)} + \frac{\lambda_c^4 (4/9)}{((\hat{s}-m_{D_o^c}^2)^2 + \Gamma_{D_o^c}^2 m_{D_o^c}^2)} \right\} \tag{3.3}$$

where $\sqrt{\hat{s}}$ is the centre-of-mass energy of the subprocess $qq \to D_o \to qq$, x_1 and x_2 are the fractions of the momenta of the incoming hadrons carried by the quarks with distributions u(x), d(x), etc., and $\Gamma_{D_o}, \Gamma_{D_o^c}$ are the decay widths of the D_o and D_o^c. No mixing between the D_o and D_o^c is taken into account in writing (3.3) and (3.2): its effects would be trivial.

In Fig. 1 we show the total cross-sections for the above process as a function of the mass m_{D_o}, assuming $m_{D_o} = m_{D_o^c}$ and $\lambda_Q = \lambda_c \equiv \lambda$ for simplicity. The common Yukawa coupling is parametrized by its ratio to the electromagnetic coupling

$$F \equiv \frac{\lambda_Q^2/4\pi}{\alpha_{em}} = \frac{\lambda_c^2/4\pi}{\alpha_{em}} \qquad (3.4)$$

Note that although neutral current constraints impose severe upper bounds on flavour- or generation-changing couplings of the D supermultiplets, there are no severe constraints on their diagonal couplings[17]. Note also that the three generations of scalar D particles could in principle have similar masses, in which case the estimated cross-sections should be increased by a factor of 3. Figure 1 includes curves for all high-energy hadron-hadron colliders currently envisaged: CERN $\bar{p}p$ at $\sqrt{s}$ = 630 GeV, FNAL $\bar{p}p$ at $\sqrt{s}$ = 1600 GeV, LHC pp at $\sqrt{s}$ = 17 TeV and SSC pp at $\sqrt{s}$ = 40 TeV.

These processes will appear experimentally as two-jet events. We have made a detailed comparison of the signal-to-background ratio at $\sqrt{s}$ = 630 GeV using data published by UA2[20]. In Table 2 we compare their $d\sigma/dM$ (jet-jet) multiplied by the widths δM of the bins they use, corresponding to their mass resolution, with the D_o cross-section we would expect for F = 1. We see that the QCD jet-jet background is between one and two orders of magnitude larger than our expected D_o cross-sections. We expect this state of affairs to be repeated at future colliders, so that it will be difficult to see the D_o in this way. Nevertheless, it would be useful for theorists if collider experiments could in the future quote directly upper limits on cross-sections for new particles decaying into jet pairs.

We turn now to the decays of the fermions $D_{\frac{1}{2}}$. In Fig. 2 we show diagrams contributing to their possible decays $D_{\frac{1}{2}} \to \bar{q}+q+\tilde{\chi}$ in leading order. The squared decay amplitude in the rest frame of the $D_{\frac{1}{2}}$ is given by:

$$|\mathcal{M}_{D_{\frac{1}{2}}}|^2 = \lambda_c^2(\sqrt{2}e)^2 4 \left\{ \frac{(1/3)^2 M_{D_{\frac{1}{2}}} E_1 \left(M_{D_{\frac{1}{2}}} E_1 + \frac{1}{2} M_{D_{\frac{1}{2}}}^2 - \frac{1}{2} m_{\tilde{\gamma}}^2\right)}{\left(P^2 - m_{\tilde{d}_R}^2\right)^2} \right.$$

$$+ \frac{(2/3)^2 M_{D_{\frac{1}{2}}} E_2 \left(M_{D_{\frac{1}{2}}} E_2 + \frac{1}{2} M_{D_{\frac{1}{2}}}^2 - \frac{1}{2} m_{\tilde{\gamma}}^2\right)}{\left(P^2 - m_{\tilde{u}_R}^2\right)^2}$$

$$\left. + \frac{(1/3)^2 M_{D_{\frac{1}{2}}} \left(M_{D_{\frac{1}{2}}} - E_1 - E_2\right) \left(M_{D_{\frac{1}{2}}} (E_1+E_2) - \frac{1}{2} M_{D_{\frac{1}{2}}}^2 + \frac{1}{2} m_{\tilde{\gamma}}^2\right)}{\left(K^2 - m_{D_o^c}^2\right)^2} \right.$$

$$-\frac{(1/3)(-2/3)M_{D_{1/2}}^2\left(2E_1E_2-M_{D_{1/2}}(E_1+E_2)+\frac{1}{2}M_{D_{1/2}}^2-\frac{1}{2}m_{\tilde{\gamma}}^2\right)}{\left(P^2-m_{\tilde{u}_R}^2\right)\qquad\left(P^2-m_{\tilde{d}_R}^2\right)}$$

$$-\frac{(1/3)(-1/3)M_{D_{1/2}}\left(M_{D_{1/2}}-2E_2\right)\left(M_{D_{1/2}}(E_1+E_2)-\frac{1}{2}M_{D_{1/2}}^2+\frac{1}{2}m_{\tilde{\gamma}}^2\right)}{\left(P^2-m_{\tilde{d}_R}^2\right)\left(K^2-m_{D_o^c}^2\right)}$$

$$+\frac{(-2/3)(-1/3)M_{D_{1/2}}\left(M_{D_{1/2}}-2E_1\right)\left(M_{D_{1/2}}(E_1+E_2)-\frac{1}{2}M_{D_{1/2}}^2+\frac{1}{2}m_{\tilde{\gamma}}^2\right)}{\left(P^2-m_{\tilde{u}_R}^2\right)\quad\left(K^2-m_{D_o^c}^2\right)}\Bigg\}$$

$$+\lambda_a^2(\sqrt{2}e)^2 4\left\{\frac{(1/3)^2\cdot 4\cdot M_{D_{1/2}}\left(M_{D_{1/2}}-E_1-E_2\right)\left(M_{D_{1/2}}(E_1+E_2)-\frac{1}{2}M_{D_{1/2}}^2+\frac{1}{2}m_{\tilde{\gamma}}^2\right)}{\left(K^2-m_{D_o}^2\right)^2}\right.$$

$$+M_{D_{1/2}}E_1\left(M_{D_{1/2}}E_1+\frac{1}{2}M_{D_{1/2}}^2-\frac{1}{2}m_{\tilde{\gamma}}^2\right)\cdot$$

$$\left(\frac{(2/3)^2}{\left(P^2-m_{\tilde{u}_L}^2\right)^2}+\frac{(-1/3)^2}{\left(P^2-m_{\tilde{d}_L}^2\right)^2}+\frac{2(2/3)(-1/3)}{\left(P^2-m_{\tilde{u}_L}^2\right)\left(P^2-m_{\tilde{d}_L}^2\right)}\right)$$

(3.5)

$$+\frac{(-1/3)\,M_{D_{1/2}}\left(M_{D_{1/2}}-2E_2\right)\left(M_{D_{1/2}}(E_1+E_2)-\frac{1}{2}M_{D_{1/2}}^2+\frac{1}{2}m_{\tilde{\gamma}}^2\right)}{\left(k^2-m_{D_0}^2\right)}\cdot$$

$$\left(\frac{(-2/3)}{\left(P^2-m_{\tilde{u}_L}^2\right)}+\frac{(1/3)}{\left(P^2-m_{\tilde{d}_L}^2\right)}\right)\Bigg\}, \qquad (3.5)$$

Contd.

where

$$P^2=M_{D_{1/2}}\left(M_{D_{1/2}}-2E_1\right),\quad k^2=2E_1E_2\left(1-\cos\phi\right)$$

ϕ is the angle between the two final-state quarks, E_1 and E_2 their energies, we have assumed that the lightest supersymmetric particle $\tilde{\chi}$ is essentially a photino $\tilde{\gamma}$ [21] and we have neglected mixing between left- and right-handed squarks. The partial decay rate d of the $D_{\frac{1}{2}}$ is given by

$$d\Gamma=\frac{1}{(2\pi)^3}\,\frac{1}{m_{D_{1/2}}}\,\left|\mathcal{M}_{D_{1/2}}\right|^2 dE_1\,dE_2 \qquad (3.6)$$

The decay rate given by (3.5) and (3.6) is a complicated function of $m_{D_{\frac{1}{2}}}/m_{\tilde{u},\tilde{d}}$. In the simplifying limit where $m_{D_{\frac{1}{2}}} \ll m_{\tilde{u},\tilde{d}}$ and neglecting quark masses and $m_{\tilde{\chi}}$, we find

$$\Gamma=\frac{1}{(2\pi)^3}M_{D_{1/2}}^5\,\frac{1}{192}\cdot\Bigg\{\lambda_c^2(\sqrt{2}e)^2 4\left(\frac{(1/3)^2}{m_{\tilde{d}_R}^4}+\frac{(-2/3)^2}{m_{\tilde{u}_R}^4}+\frac{(1/3)(-2/3)2}{m_{\tilde{d}_R}^2\,m_{\tilde{u}_R}^2}\right)$$

$$-\lambda_Q^2(\sqrt{2}e)^2 4\left(\frac{(-1/3)^2}{m_{\tilde{d}_L}^4}+\frac{(2/3)^2}{m_{\tilde{u}_L}^4}+\frac{(-1/3)(2/3)2}{m_{\tilde{u}_L}^2\,m_{\tilde{d}_L}^2}\right)\Bigg\} \qquad (3.7)$$

Rather than use (3.5) in calculating the missing energy signature for $D_{\frac{1}{2}}$ production discussed in Section 4, we use simple phase space. We do not expect our results to be sensitive to this simplification.

3.3 Couplings to Quarks and Leptons

We now turn to the case (3.1b). Mixing of the D particles with conventional charge -1/3 quarks would be possible if $\langle 0|\tilde{\nu}|0\rangle \neq 0$. However, as mentioned earlier, this possibility is severely constrained by experiment, and we assume $\langle 0|\tilde{\nu}|0\rangle = 0$, in which case there is no D/d mixing. Single production of the scalar D is possible in ep collisions via $e^-u \to D_o/\bar{D}_o^c (e^+\bar{u} \to D_o^c/\bar{D}_o)$, while $D_o/\bar{D}_o^c \to q+\ell$ ($D_o^c/\bar{D}_o \to \bar{q}+\bar{\ell}$) decays dominate. The squared amplitudes for these decays are

$$|\mathcal{M}_{D_o}|^2 = 6\lambda_e^2 m_{D_o}^2 \quad , \quad |\mathcal{M}_{D_o^c}|^2 = 12\lambda_L^2 m_{D_o^c}^2 \, . \tag{3.8}$$

Neglecting mixing, all of the D_o decays are to jets + charged leptons, while the D_o^c has 50% branching ratios into (jets + charged leptons) and (jets + neutrinos). Again, we have no idea what the ratio of the couplings λ_ℓ and λ_L might be. The cross-section for the process $ep \to D_o \to \ell q$ is given by

$$d\sigma = \frac{d\hat{s}}{16\pi} \cdot \frac{\hat{s}}{s} \left\{ u\left(\frac{\hat{s}}{s}\right) + \cdots \right\} \cdot$$

$$\left\{ \frac{2\lambda_L^4}{(\hat{s}-M_{D^c}^2)^2 + \Gamma_{D^c}^2 M_{D^c}^2} + \frac{\lambda_e^4}{(\hat{s}-M_D^2)^2 + \Gamma_D^2 M_D^2} \right\} \tag{3.9}$$

where $\sqrt{s} = \sqrt{4E_e E_p}$ is the centre-of-mass energy and $\hat{s}$ is the invariant mass squared of the colliding lepto-quark combination. In Fig. 3 we show the integrated cross-section as a function of m_{D_o}, assuming $m_{D_o} = m_{D_o^c}$ and $(\lambda_L^2+\lambda_e^2) = \lambda^2 = 4\pi . F . \alpha_{em}$ as in Eq. (3.4). Results are presented for HERA: $\sqrt{s}$ = 314 GeV, and for two LHC/LEP options: $\sqrt{s}$ = 1.4 TeV, 1.8 TeV.

These processes will appear experimentally as (lepton + jet) final states. The cases where the lepton is an electron must be compared with the background from the conventional process e+p → e+X, whereas the cases where the lepton is a

neutrino must be compared with the charged current cross-sections for $e+p \to \nu+X$. There would be relatively little background if the D_o decays into a μ or a τ, but flavour-changing neutral current constraints[17] severely restrict the possible couplings to these leptons.

We show in Table 3 numerical calculations of the cross-sections for $e^-+p \to (D_o \to e^-+q) + X$, compared with the continuum background coming from the conventional electromagnetic and neutral current scattering $e^-+p \to e^-+X$. To estimate the background, we have integrated over bins in x corresponding to the e + jet mass resolutions expected for the HERA detector ZEUS[22]. We see that the signal-to-background ratios are very favourable if F = 1, which may be an upper bound on the $Dq\ell$ coupling. It should also be possible to detect the D_o even if F is considerably smaller than one. The process $e+q \to D_o \to \nu+q$ can be detected almost equally easily. The background from the Standard Model charged current reaction is slightly smaller than that shown in Table 3. The resolution for the mass bump in the $(\nu+q)$ channel is in the ZEUS detector only a factor ~ 1.6 worse than in the $(e+q)$ channel. The other HERA detector H1 is expected to have an $(e+q)$ mass resolution somewhat better (by a factor ~ 1.1) and a $(\nu+q)$ mass resolution somewhat worse (by a factor ~ 1/1.7) than the ZEUS detector. Similar calculations can be made for higher energy ep collider projects, with similar conclusions[23].

The squared amplitude for $D_{\frac{1}{2}} \to q\ell\tilde{\chi}$ decay in the $D_{\frac{1}{2}}$ rest frame is given by

$$|\mathcal{M}|^2_{D_{1/2}} = \lambda_L^2(\sqrt{2}e)^2 \cdot 12 \cdot \left\{ \frac{M_{D_{1/2}} E_q \left(\frac{1}{2} M^2_{D_{1/2}} - \frac{1}{2} m^2_{\tilde{\gamma}} - M_{D_{1/2}} E_q\right)}{\left(P^2 - m^2_{\tilde{e}_L}\right)^2} + \right.$$

$$\left(\frac{1}{2} M^2_{D_{1/2}} - \frac{1}{2} m^2_{\tilde{\gamma}} - M_{D_{1/2}} E_\ell\right) M_{D_{1/2}} E_\ell \left[\frac{(2/3)^2}{\left(P^2 - m^2_{\tilde{u}_L}\right)^2} + \frac{(1/3)^2}{\left(P^2 - m^2_{\tilde{d}_L}\right)^2} \right] +$$

$$\left. \frac{2 \cdot (1/3)^2 M_{D_{1/2}} \left(M_{D_{1/2}} - E_q - E_\ell\right) \left(M_{D_{1/2}} (E_\ell + E_q) - \frac{1}{2} M^2_{D_{1/2}} + \frac{1}{2} m^2_{\tilde{\gamma}}\right)}{\left(K^2 - m^2_{D^c_o}\right)^2} + \right.$$

$$\frac{(2/3)\left(2M_{D_{1/2}}^2 E_\ell E_q - M_{D_{1/2}}^2\left(M_{D_{1/2}}(E_\ell+E_q) - \frac{1}{2}M_{D_{1/2}}^2 + \frac{1}{2}m_{\tilde{\gamma}}^2\right)\right)}{\left(P^2 - m_{\tilde{u}_L}^2\right)\qquad\left(P^2 - m_{\tilde{e}_L}^2\right)} +$$

$$\frac{(1/3)\,M_{D_{1/2}}\left(M_{D_{1/2}}(E_\ell+E_q) - \frac{1}{2}M_{D_{1/2}}^2 + \frac{1}{2}m_{\tilde{\gamma}}^2\right)}{\left(K^2 - m_{D_0^c}^2\right)} \cdot$$

$$\left[\frac{M_{D_{1/2}} - 2E_q}{\left(P^2 - m_{\tilde{e}_L}^2\right)} + \frac{(M_{D_{1/2}} - 2E_\ell)(1/3)}{\left(P^2 - m_{\tilde{d}_L}^2\right)} + \frac{(M_{D_{1/2}} - 2E_\ell)(-2/3)}{\left(P^2 - m_{\tilde{u}_L}^2\right)}\right]\Bigg\} +$$

$$\lambda_e^2 (\sqrt{2}e)^2 \cdot 12 \cdot \Bigg\{ \frac{(-2/3)^2 M_{D_{1/2}} E_\ell\left(\frac{1}{2}M_{D_{1/2}}^2 - \frac{1}{2}m_{\tilde{\gamma}}^2 - M_{D_{1/2}} E_e\right)}{\left(P^2 - m_{\tilde{u}_R}^2\right)^2} +$$

$$\frac{M_{D_{1/2}} E_q\left(\frac{1}{2}M_{D_{1/2}}^2 - \frac{1}{2}m_{\tilde{\gamma}}^2 - M_{D_{1/2}} E_q\right)}{\left(P^2 - m_{\tilde{e}_R}^2\right)^2} -$$

$$\frac{(-2/3)\left(2M_{D_{1/2}}^2 E_e E_q - M_{D_{1/2}}^2\left(M_{D_{1/2}}(E_\ell+E_q) - \frac{1}{2}M_{D_{1/2}}^2 + \frac{1}{2}m_{\tilde{\gamma}}^2\right)\right)}{\left(P^2 - m_{\tilde{e}_R}^2\right)\qquad\left(P^2 - m_{\tilde{u}_R}^2\right)} +$$

(3.10)

$$\left.\frac{(1/3)^2 M_{D_{1/2}}\left(M_{D_{1/2}}-E_q-E_\ell\right)\left(M_{D_{1/2}}(E_\ell+E_q)-\frac{1}{2}M_{D_{1/2}}^2+\frac{1}{2}m_{\tilde{\gamma}}^2\right)}{\left(K^2-m_{D_0}^2\right)^2}\right\} \quad (3.10)\ \text{Contd.}$$

where

$$P^2 = M_{D_{1/2}}\left(M_{D_{1/2}}-2E_{\ell,q}\right)$$

$$K^2 = 2E_\ell E_q\left(1-\cos\omega\right)$$

ω is the angle between the final-state quark and lepton, E_q and E_ℓ are their energies and $d\Gamma$ is given again by (3.6). In the simplifying limit where $m_{D_{\frac{1}{2}}} \ll m_{\tilde{\chi}}, m_{\tilde{q}}$, we find

$$\Gamma = \frac{1}{(2\pi)^3}\cdot\frac{M_{D_{1/2}}^5}{192}\left\{\lambda_L^2(\sqrt{2}e)^2\cdot 3\cdot 4\left(\frac{1}{m_{\tilde{e}_L}^4}-\frac{(2/3)^2}{m_{\tilde{u}_L}^4}-\frac{(-1/3)^2}{m_{\tilde{d}_L}^4}-\frac{2(2/3)^2}{m_{\tilde{u}_L}^2 m_{\tilde{e}_L}^2}\right)\right.$$

$$\left.+\lambda_e^2(\sqrt{2}e)^2\cdot 3\cdot 4\left(\frac{(-2/3)^2}{m_{\tilde{u}_R}^4}+\frac{1}{m_{\tilde{e}_R}^4}+\frac{2(-2/3)}{m_{\tilde{e}_R}^2 m_{\tilde{u}_R}^2}\right)\right\} \quad (3.11)$$

which is used in calculating signatures for $D_{\frac{1}{2}}$ production in Section 4.

3.4 Couplings to Conjugate Neutrinos

Finally, we turn to the case (3.1c). Mixing of the D particles with conventional charge -1/3 quarks would be possible if $\langle 0|\tilde{\nu}^c|0\rangle \neq 0$. However, as mentioned before, we assume here that $\langle 0|\tilde{\nu}^c|0\rangle = 0$ and hence that there is no D/d mixing. In this case there is no single production of the D_o in either hadron-hadron or electron-hadron collisions. The dominant decays of the D_o are to $q+\nu^c$,

which would have the same experimental missing-energy signature as conventional squark $\tilde{q} \to q+\tilde{\gamma}$ decay. The dominant decays of the $D_{\frac{1}{2}}$ in this case are to $q+\nu^c+\tilde{\chi}$ via the squared amplitude

$$|\mathcal{M}|^2 = \lambda_\nu^2 (\sqrt{2}e)^2 \cdot 12 \cdot \frac{(\frac{1}{3})^2 M_{D_{\frac{1}{2}}} E_\nu \left(\frac{1}{2} M_{D_{\frac{1}{2}}}^2 - \frac{1}{2} m_{\tilde{\gamma}}^2 - M_{D_{\frac{1}{2}}} E_\nu\right)}{\left(P^2 - m_{\tilde{u}_R}^2\right)^2},$$

$$P^2 = M_{D_{\frac{1}{2}}} \left(M_{D_{\frac{1}{2}}} - 2E_\nu\right) \qquad (3.12)$$

where we have already taken the simplifying limit $m_{D_{\frac{1}{2}}} << m_{\tilde{\chi}}, m_{\tilde{q}}$ which is used in the phenomenological analysis of its missing energy signature in Section 4.

4. - PAIR PRODUCTION IN HADRON-HADRON COLLISIONS

In this section we discuss the possible cross-sections and signatures for $\overset{(-)}{p}p \to D_o\bar{D}_o+X$ and $D_{\frac{1}{2}}\bar{D}_{\frac{1}{2}}+X$.

4.1 Cross-sections

The forms of the parton-parton cross-sections for gg, $\bar{q}q \to D_o\bar{D}_o$ are identical to those of gg, $\bar{q}q \to \tilde{q}\bar{\tilde{q}}$ [24] if one compares the limits $m_{D_{\frac{1}{2}}} >> m_{D_o}$ and $m_{\tilde{g}} >> m_{\tilde{q}}$, due to the fact that D_o couplings to gluons are identical to those of $\tilde{q}$. The only difference between the total cross-sections in these limits is therefore an overall combinatorial factor counting the total number of D_o or $\tilde{q}$ species. In previous work, two of us [25] have generally assumed 5 approximately degenerate flavours of squark ($\tilde{u}$, $\tilde{d}$, $\tilde{s}$, $\tilde{c}$ and $\tilde{b}$) and added together both left- and right-handed quarks. Here we add together the D_o scalars expected from three generations, and also include both left- and right-handed states. In this case, $\sigma(D_o\bar{D}_o)/\sigma(\tilde{q}\bar{\tilde{q}}) = 3/5$.

The forms of the parton-parton cross-sections for gg, $\bar{q}q \to D_{\frac{1}{2}}\bar{D}_{\frac{1}{2}}$ are identical to those of gg, $\bar{q}q \to t\bar{t}$ [26] if one considers the limit $m_{D_o} >> m_{D_{\frac{1}{2}}}$. Equivalently, these parton-parton cross-sections can be obtained from those for gg, $\bar{q}q \to \tilde{g}\tilde{g}$ [24] in the limit $m_{\tilde{q}} >> m_{\tilde{g}}$ simply by adjusting the colour factors.

4.2 Possible Signatures

As discussed in the previous section, possible decays of the D_o are to $q\nu$, $q\ell^-$ and $\bar{q}\bar{q}$, while the $D_{\frac{1}{2}}$ may decay to $q\nu\tilde{\chi}$, $q\ell^-\tilde{\chi}$ or $\bar{q}\bar{q}\tilde{\chi}$, where the $\tilde{\chi}$ is a weakly-interacting neutral Majorana fermion similar to the photino, which can carry off missing energy. We therefore have the following possible event signatures:

Missing energy: $D_o\bar{D}_o \rightarrow (q\nu)(\bar{q}\bar{\nu})$
$D_{\frac{1}{2}}\bar{D}_{\frac{1}{2}} \rightarrow (\bar{q}\bar{q}\tilde{\chi})(qq\tilde{\chi})$ or $(q\nu\tilde{\chi})(\bar{q}\bar{\nu}\tilde{\chi})$

Charged lepton pairs: $D_o\bar{D}_o \rightarrow (q\ell^-)(\bar{q}\ell^+)$

Leptons and missing energy: $D_{\frac{1}{2}}\bar{D}_{\frac{1}{2}} \rightarrow (q\ell^-\tilde{\chi})(\bar{q}\ell^+\tilde{\chi})$

Dijet mass bumps: $D_o\bar{D}_o \rightarrow (\bar{q}\bar{q})(qq)$

While the semileptonic decay of one D is not compatible with the simultaneous hadronic decay of another D, it is in principle possible to mix the semileptonic decay into a charged lepton of one D with the neutrino decay of another D. However, we will not discuss such dijet + lepton + missing energy final states. Nor will we discuss final states with two charged leptons of different flavours: $e^{\pm}\mu^{\mp}$, $e^{\pm}\tau^{\mp}$, $\mu^{\pm}\tau^{\mp}$. We concentrate on the missing-energy signatures and on the charged lepton pair signatures. We present here results for $\bar{p}p$ collisions at $\sqrt{s}$ = 630 GeV corresponding to the CERN Collider, and 1600 GeV, corresponding to the Fermilab Collider: results for pp collisions at $\sqrt{s}$ = 17 TeV corresponding to the LHC will be presented elsewhere[23].

4.3 Missing Energy Signatures

To discuss these quantitatively we have used the same approach as in previous work[25] on UA1 data[14]. We divide missing energy events into the following categories; monojets: only one cluster of hadronic energy within $\Delta R = \sqrt{(\Delta\phi)^2+(\Delta\eta)^2} = 1$ above a threshold of E_T = 12 GeV, and missing transverse momentum p_T in excess of 4σ, where the measurement error $\sigma = 0.7\sqrt{E_T(GeV)}$; dijets: two such jet clusters and $p_T > 4\sigma$; trijets: three such jets, etc. Our calculations include a somewhat more subtle characterization of the UA1 detector which is described in previous publications[25]. However, a full description of the

assignments of missing energy events to different categories is impossible in the absence of a full detector simulation. Therefore in this paper we restrict ourselves to quoting cross-sections for monojet events and multijet events, and emphasize that a realistic detector may shuffle events between these two categories.

$D_o \to q\nu$ The signature for this decay is identical to that previously discussed [13] for $\tilde{q} \to q\tilde{\gamma}$ with $m_{\tilde{\gamma}} = 0$. Figure 4a contains our predictions for monojets and multijets*) from $D_o\bar{D}_o$ production at $\sqrt{s} = 630$ GeV including the factor of 3/5 in the cross-section which was mentioned previously. The horizontal lines correspond to $\sigma = 7$ pb (solid line: five events in the present event sample of about 700 nb^{-1}), $\sigma = 1.4$ pb (dashed line: corresponding to one event in the present sample) and $\sigma = 0.28$ pb^{-1} [dotted line: corresponding to perhaps five events at the $\bar{p}p$ collider with ACOL[27]]. We believe that a lower limit on the D_o mass could only be established by the UA1 collaboration itself. If it would establish an upper limit of five multijet events in the present data, that would correspond to $m_{D_o} \gtrsim 60$ to 70 GeV. Figure 4b contains analogous cross-section curves for $\sqrt{s} = 1600$ GeV. At this energy, a sensitivity comparable to present CERN Collider data would increase the possible limit to $m_{D_o} \gtrsim 120$ to 130 GeV.

$D_{\frac{1}{2}} \to q\nu\tilde{\chi}$ Here there is some additional ambiguity provided by the unknown mass of the $\tilde{\chi}$. Model analyses of sparticle spectra suggest that $m_{\tilde{\chi}} \gtrsim 15$ GeV, and it would easily be a large fraction of $m_{D_{\frac{1}{2}}}$. Therefore we plot in Fig. 5a our results for $\sqrt{s} = 630$ GeV as contours in the $(m_{D_{\frac{1}{2}}}, m_{\tilde{\chi}})$ plane corresponding to $\sigma = 7$ pb (solid lines), 1.4 pb (dashed lines) and 0.28 pb (dotted lines) as in Fig. 4a. Naïve interpolation between these contours will give cross-sections accurate to better than a factor of 2, which is in any case the expected accuracy of our calculations. We see that monojet events are always more copious than multijet events. We also see from Fig. 5 that the UA1 sensitivity to $m_{D_{\frac{1}{2}}}$ is essentially unchanged for $0 \leq m_{\tilde{\chi}} \leq 15$ GeV, but decreases significantly for larger $m_{\tilde{\chi}}$, and disappears in the limit $m_{\tilde{\chi}} \to m_{D_{\frac{1}{2}}}$. Less than five monojet events in the present UA1 data[14] would correspond to $m_{D_{\frac{1}{2}}} \gtrsim 70$ GeV if the $\tilde{\chi}$ is light, or $m_{D_{\frac{1}{2}}} \gtrsim 50$ to 60 GeV if $m_{\tilde{\chi}} = \frac{1}{2} m_{D_{\frac{1}{2}}}$. We plot in Fig. 5b cross-section curves for $\sqrt{s} = 1600$ GeV assuming for definiteness that $m_{\tilde{\chi}} = \frac{1}{2} m_{D_{\frac{1}{2}}}$. We see that a sensitivity comparable to present UA1 data would increase the possible limit to $m_{D_{\frac{1}{2}}} \gtrsim 120$ GeV.

---

*) Note that in this and the next case the vast majority of multijet events only contain two jets.

$D_{\frac{1}{2}} \to \bar{q}q\tilde{\chi}$ This is an alternative decay mode of the $D_{\frac{1}{2}}$ which has a signature similar to the conventional $\tilde{g} \to q\bar{q}\tilde{\gamma}$ decay, although the cross-section is somewhat different and the mass of the $\tilde{\chi}$ may not be negligible. In Fig. 6a we have plotted for $\sqrt{s}$ = 630 GeV contours in the $(m_{D_{\frac{1}{2}}}, m_{\tilde{\chi}})$ plane corresponding to σ = 7 pb (solid lines), 1.4 pb (dashed lines) and 0.28 pb (dotted lines) as in Fig. 5a. We see that the multijet cross-sections are larger for low $m_{\tilde{\chi}}$ and large $m_{D_{\frac{1}{2}}}$, while the multijet cross-sections are larger for bigger $m_{\tilde{\chi}}$. Thus monojet and multijet searches to some extent complement each other. An upper limit of five multijet events in the present data would correspond to $m_{D_{\frac{1}{2}}} \gtrsim 80$ GeV for $m_{\tilde{\chi}} \lesssim 20$ GeV, while an upper limit of five monojet events in the present data would correspond to $m_{D_{\frac{1}{2}}} \gtrsim 60$ GeV if $m_{\chi} = \frac{1}{2} m_{D_{\frac{1}{2}}}$. Cross-section curves for $\sqrt{s}$ = 1600 GeV and $m_{\tilde{\chi}} = \frac{1}{2} m_{D_{\frac{1}{2}}}$ are plotted in Fig. 6b. Here we see that a multijet sensitivity comparable to that presently achieved by UA1 would reach $m_{D_{\frac{1}{2}}} \sim 150$ GeV.

4.4 Charged Lepton Signatures

Taking our cue again from UA1[15], we have taken the following cuts on charged leptons: $|\eta_1| < 1.3$, $|\eta_2| < 2.0$, $m_{\ell^+\ell^-} > 6$ GeV and $p_T^{\ell 1}$, $p_T^{\ell 2} > 3$ GeV for muons, $p_T^{\ell 1}$, $p_T^{\ell 2} > 8$ GeV for electrons. We have also tried the effects of isolation cuts: $(\Sigma_{1,2} E_T^2) < 9$ GeV^2 in the combination of cores with $\Delta R \equiv \sqrt{(\Delta\phi)^2+(\Delta\eta)^2} < 0.7$ around the two charged leptons. Thus we quote cross-sections for $(\mu^+\mu^-)$ both total and isolated, and similarly for (e^+e^-) pairs.

$D_o \to q\ell$ Our results at $\sqrt{s}$ = 630 GeV are shown in Fig. 7a. The total (solid line) and isolated (dashed line) curves are for $\mu^+\mu^-$ pairs. The e^+e^- cross-sections are indistinguishable for $m_{D_o} > 60$ GeV and differ by less than 10% even for m_{D_o} = 40 GeV. Note that here we have assumed a 100% branching ratio into $q\mu^-$ for each of the three generations of D_o particles. This is probably unreasonable, a better guess being that at most one of the three generations of D_o particles would have a large branching ratio into $q\mu^-$. In this case, the cross-sections in Fig. 7 should be reduced by a factor of 3. Taking this point of view, an upper limit of five events in the present UA1 event sample[15] would correspond to $m_{D_o} \gtrsim 60$ to 70 GeV. Corresponding cross-sections for $\sqrt{s}$ = 1600 GeV are shown in Fig. 7b. A sensitivity comparable to UA1's present achievement would then yield $m_{D_o} \gtrsim 140$ GeV.

$D_{\frac{1}{2}} \to q\ell\tilde{\chi}$ Here we meet again the ambiguity in the mass of the $\tilde{\chi}$. If these events

are treated simply as possible missing energy events, and no attempt is made to identify the charged leptons, then the results of Fig. 6 are directly applicable. Alternatively, they could be analyzed as $(\ell^+\ell^-)$ events with no attempt made to measure missing energy. In this case, their signature would be similar to that of $D_o \to q\ell$. Figures 8a and 8b show cross-section curves at $\sqrt{s}$ = 630 GeV and 1600 GeV respectively, assuming $m_{\tilde{\chi}} = \frac{1}{2}m_{D_{\frac{1}{2}}}$. We see from Fig. 8a that an upper bound of five events in the present UA1 sample would yield $m_{D_{\frac{1}{2}}} \gtrsim 80$ GeV, while comparable sensitivity at the Fermilab Collider would yield $m_{D_{\frac{1}{2}}} \gtrsim 160$ GeV.

5. - CONCLUSIONS

Superstring-inspired models offer the possibility that additional light colour-triplet, charge $|1/3|$ particles exist in addition to conventional quarks. These D particles exist with spin zero (two per generation) and spin $\frac{1}{2}$ (one Dirac fermion per generation). We have motivated and studied the case where the D particles do not mix with the conventional charge $|1/3|$ quarks d,s,b. In contrast to conventional GUTs, symmetry breaking by the Hosotani mechanism at the compactification scale offers the possibilities that D particles have <u>either</u> purely leptoquark couplings $Dq\bar{\ell}$, <u>or</u> purely diquark couplings Dqq. In this paper we have studied the phenomenologies of these two cases.

In the case of leptoquark couplings, we find that the spin-zero D_o particles could be produced and observed at HERA if they have masses $\lesssim$ 250 GeV. Future ep colliders could extend the search for leptoquark D_o particles above 1 TeV.

In the case of diquark couplings, we find that the single production of spin-zero D_o particles at hadron-hadron colliders through qq annihilation is likely to be overwhelmed by a large QCD jet-jet background.

Pair production of $D_o\bar{D}_o$ and $D_{\frac{1}{2}}\bar{D}_{\frac{1}{2}}$ at hadron-hadron colliders offers a promising way to search for these particles. The pair-production mechanism leads to characteristic experimental signatures in almost all possible decay channels if $m_{\tilde{\chi}}/m_D < \frac{1}{2}$. The D_o and $D_{\frac{1}{2}}$ particles could be sought in samples of missing-energy events, $\ell^+\ell^-$ events and top candidates. The present CERN $p\bar{p}$ Collider probably has sensitivity to these particles if they have masses $\lesssim$ 60 to 70 GeV. The improved luminosity available with ACOL would increase this range to about 100 GeV. The FNAL Tevatron Collider should be able to see D_o or $D_{\frac{1}{2}}$ particles weighing up to ~ 150 GeV. In the longer term, at the LHC or the SSC one could search for

the pair production of D_0 and $D_{\frac{1}{2}}$ particles with masses $\lesssim$ 2 TeV, as has previously been discussed for squark and gluino searches.

We hope that this paper stimulates our experimental colleagues to search systematically in their present and future data for exotic charge $|1/3|$ particles with diquark or leptoquark couplings.

ACKNOWLEDGEMENTS

One of us (F.Z.) is partially supported by "Fondazione Ing. Aldo Gini". Another of us (V.D.A.) wishes to thank the Ministry of National Economy of Greece for financial support.

We would also like to thank our experimental colleagues, especially M. Della Negra and F. Pauss, for valuable discussions.

0.2	$\lesssim$	$\bar{v}/v$	$\lesssim$	0.6
2.8	$\lesssim$	x/v	$\lesssim$	10
100 GeV	$\lesssim$	$m_{\frac{1}{2}}$	$\lesssim$	500 GeV
0.15	$\lesssim$	λ_{333}	$\lesssim$	0.35
3.00	$\lesssim$	$\tilde{m}^2_{D_3}/m^2_{\frac{1}{2}}$	$\lesssim$	3.35
2.95	$\lesssim$	$\tilde{m}_{D_3^c}{}^2/m^2_{\frac{1}{2}}$	$\lesssim$	3.30
-3.5	$\lesssim$	$A^k_{333}/m_{\frac{1}{2}}$	$\lesssim$	-3.0
0.25	$\lesssim$	k_{333}	$\lesssim$	0.55

Table 1

Typical values[6] of the model parameters, specified at the electroweak symmetry-breaking scale. The couplings k_{aa3} (a = 1,2) are assumed to be significantly smaller than the coupling k_{333}.

$\sqrt{s}$ = 630 GeV

m (GeV)	125	145	168	188	208	228	268	288
δm (GeV)	11.0	12.3	13.7	14.9	16.2	17.3	19.5	20.6
$d\sigma/dm$ (nb/GeV)	3.10^{-1}	9.10^{-2}	3.10^{-2}	10^{-2}	7.10^{-3}	3.10^{-3}	4.10^{-4}	6.10^{-4}
$\delta\sigma$ (nb)	3.3	1.11	0.41	0.15	0.11	0.05	$7.8.10^{-3}$	12.10^{-3}
σ(nb) F = 1	$0.8.10^{-1}$	$0.3.10^{-1}$	$0.1.10^{-1}$	$0.5.10^{-2}$	$0.2.10^{-2}$	$0.9.10^{-3}$	$0.2.10^{-3}$	$0.6.10^{-4}$

Table 2: Signal and Background for D_o Search in $\bar{p}p$ Collisions

We have assumed, following UA2[20], that the mass resolution $\delta m = 0.29[m(GeV)]^{3/4}$ and computed $\delta\sigma = 2\delta m d\sigma/dm$

m_{D_o}	100	200	300
$x = m_D^2/s$	0.1	0.40	0.91
Background cross-sections $d\sigma/dx$ e_L^-(nb)	42.3	1.4	$2.0.10^{-4}$
e_R^-(nb)	24.6	0.7	$9.3.10^{-5}$
δm(GeV) ZEUS[22]	2.05	2.9	3.5
$\delta\sigma = 4m\delta m\sigma/s$(nb) (ZEUS)[22]	(L) 0.35 (R) 0.20	0.032 0.016	$8.4.10^{-6}$ $3.9.10^{-6}$
σ_{D_o} (F = 1) (nb)	3.6	0.32	$0.83.10^{-4}$

Table 3: Signal and Background for D_o Search in ep Collisions

Calculations for HERA: $\sqrt{s}$ = 314 GeV, corresponding to E_e = 30 GeV, E_p = 820 GeV

REFERENCES

1) For reviews, see:
J. Ellis, CERN preprints TH.4439 and TH.4474 (1986);
L. Ibanez, CERN preprint TH.4444 (1986);
H.P. Nilles, CERN preprint TH.4459 (1986);
G. Segrè, University of Pennsylvania preprint "Superstrings and Four-Dimensional Physics" (1986).

2) P. Candelas, G.T. Horowitz, A. Strominger and E. Witten, Nucl. Phys. B258 (1985) 46.

3) E. Witten, Nucl. Phys. B258 (1985) 75;
M. Dine, V. Kaplunovsky, M. Mangano, C. Nappi and N. Seiberg, Nucl. Phys. B259 (1985) 549;
J.D. Breit, B.A. Ovrut and G. Segrè, Phys. Lett. 158B (1985) 33;
S. Cecotti, J.-P. Derendinger, S. Ferrara, L. Giradello and M. Roncadelli, Phys. Lett. 156B (1985) 318.

4) L. Dixon, J.A. Harvey, C. Vafa and E. Witten, Nucl. Phys. B261 (1985) 678; Nucl. Phys. B274 (1986) 285.

5) B.A. Campbell, J. Ellis and D.V. Nanopoulos, Phys. Lett. 181B (1986) 283.

6) E. Cohen, J. Ellis, K. Enqvist and D.V. Nanopoulos, Phys. Lett. 165B (1985) 76;
J. Ellis, K. Enqvist, D.V. Nanopoulos and F. Zwirner, Mod. Phys. Lett. A1 (1986) 57 and Nucl. Phys. B276 (1986) 14.

7) V. Barger, N. Deshpande and K. Whisnant, Phys. Rev. Lett. 56 (1986) 30;
L.S. Durkin and P. Langacker, Phys. Lett. 166B (1986) 436;
F. Del Aguila, G. Blair, M. Daniel and G.G. Ross, CERN preprint TH.4376 (1986);
D. London and J. Rosner, Phys. Rev. D34 (1986) 1530;
F. Costa, J. Ellis, G.L. Fogli, D.V. Nanopoulos and F. Zwirner, in preparation.

8) F. Del Aguila, M. Quiros and F. Zwirner, CERN preprints TH.4506 and TH.4536 (1986);
B. Adeva, F. Del Aguila, D.V. Nanopoulos, M. Quiros and F. Zwirner, CERN preprint TH.4535 (1986);
V. Barger, N.G. Deshpande, J.L. Rosner and K. Whisnant, University of Wisconsin preprint MAD/PH/299 (1986).

9) J. Ellis, D.V. Nanopoulos, S.T. Petcov and F. Zwirner, Nucl. Phys. B283 (1987) 83;
H.L. Haber and M. Sher, University of California, Santa Cruz preprint SCIPP 86/66 (1986);
V. Barger and W.-Y. Keung, Phys. Rev. D34 (1986) 2902.

10) J.L. Rosner, Comm. Nucl. Part. Phys. 15 (1986) 195.
R. Robinett, Phys. Rev. D33 (1986) 1908;
V. Barger et al., Phys. Rev. D33 (1986) 1912.

11) Y. Hosotani, Phys. Lett. 129B (983) 193.

12) B.A. Campbell, J. Ellis and D.V. Nanopoulos, Phys. Lett. 141B (1984) 229.

13) For a review and references, see:
J. Ellis, Proc. 1985 Int. Symp. on Lepton and Photon Interactions at High Energies, Kyoto 1985, eds. M. Konuma and K. Takahashi (Kyoto Univ., 1985), p. 850.

14) UA1 Collaboration, G. Arnison et al., Phys. Lett. 139B (1984) 115.

15) UA1 Collaboration, G. Arnison et al., in preparation.

16) UA1 Collaboration, G. Arnison et al., Phys. Lett. 147B (1984) 493.

17) B.A. Campbell, J. Ellis, M.K. Gaillard, D.V. Nanopoulos and K.A. Olive, Phys. Lett. 180B (1986) 77;
B.A. Campbell, J. Ellis, K. Enqvist, M.K. Gaillard and D.V. Nanopoulos, CERN preprint TH.4473 (1986).

18) H. Georgi and D.V. Nanopoulos, Phys. Lett. 82B (1979) 95.

19) J. Ellis, D.V. Nanopoulos, M. Quiros and F. Zwirner, Phys. Lett. 180B (1986) 83.

20) UA2 Collaboration, P. Bagnaia et al., in preparation.

21) B.A. Campbell, J. Ellis, K. Enqvist, J.S. Hagelin, D.V. Nanopoulos and K.A. Olive, Phys. Lett. 173B (1986) 270.

22) ZEUS Collaboration, technical proposal (1986).

23) "Physics Beyond the Standard Model" Working Group, Workshop on Physics at Future Accelerators, La Thuile (1987).

24) G.L. Kane and J. Leveillé, Phys. Lett. 112B (1982) 227;
P. Harrison and C.H. Llewellyn Smith, Nucl. Phys. B213 (1982) 223; B223 (1983) 542.

25) J. Ellis and H. Kowalski, Phys. Lett. 142B (1986) 441; Nucl. Phys. B246 (1986) 189 and B259 (1985) 109.

FIGURE CAPTIONS

Fig. 1 : Total cross-sections, as functions of m_{D_o} and $F \equiv (\lambda^2/4\pi)/\alpha_{em}$, for the process $h+h \to (D \to qq)+X$ for a) $\bar{p}p$ at $\sqrt{s}$ = 630 GeV, b) $\bar{p}p$ at $\sqrt{s}$ = 1600 GeV, c) pp at $\sqrt{s}$ = 17 TeV and d) pp at $\sqrt{s}$ = 40 TeV. The cross-sections include D_o, D_o^c, $\bar{D}_o$ and $\bar{D}_o^c$ production.

Fig. 2 : Tree diagrams contributing to the decay $D_{\frac{1}{2}} \to \bar{q}\bar{q}\tilde{\chi}$.

Fig. 3 : Total cross-section, as a function of m_{D_o} and $F \equiv (\lambda^2/4\pi)/\alpha_{em}$, for the process $ep \to (D \to lq)+X$; a) at $\sqrt{s}$ = 314 GeV, b) at $\sqrt{s}$ = 1.4 TeV and c) at $\sqrt{s}$ = 1.8 TeV. The cross-sections include D_o and $\bar{D}_o^c$ production.

Fig. 4 : Total cross-section, as a function of m_{D_o}, for the process
$\bar{p}p \to (D_o \to q\nu) + (\bar{D}_o \to \bar{q}\bar{\nu}) + X$, $(D_o^c \to \bar{q}\bar{\nu}) + (\bar{D}_o^c \to q\nu) + X$
a) at $\sqrt{s}$ = 630 GeV and b) at $\sqrt{s}$ = 1600 GeV.

Fig. 5 : a) Contours, in the $(M_{D_{\frac{1}{2}}}, m_{\tilde{\chi}})$ plane, of σ = 7pb (solid line), σ = 1.4pb (dashed line) and σ = 0.28pb (dotted line), for monojet (circles) and multijet (crosses) events from the process
$\bar{p}p \to (D_{\frac{1}{2}} \to q\nu\tilde{\chi}) + (\bar{D}_{\frac{1}{2}} \to \bar{q}\bar{\nu}\tilde{\chi}) + X$ at $\sqrt{s}$ = 630 GeV;

b) total cross-section as a function of $m_{D_{\frac{1}{2}}}$ (assumed equal to $2m_{\tilde{\chi}}$), for the same process at $\sqrt{s}$ = 1600 GeV.

Fig. 6 a) As in Fig. 5a for the process
$\bar{p}p \to (D_{\frac{1}{2}} \to \bar{q}\bar{q}\tilde{\chi}) + (\bar{D}_{\frac{1}{2}} \to q\bar{q}\tilde{\chi}) + X$ at $\sqrt{s}$ = 630 GeV;
b) as in Fig. 5b for the same process.

Fig. 7 : Total cross-section as a function of m_{D_o} for the process
$\bar{p}p \to (D_o \to q\mu^-) + (\bar{D}_o \to \bar{q}\mu^+) + X$, $(D_o^c \to \bar{q}\mu^+) + (\bar{D}_o^c \to q\mu^-) + X$
a) at $\sqrt{s}$ = 630 GeV and b) at $\sqrt{s}$ = 1600 GeV. The centrality and isolation cuts are specified in the text.

Fig. 8 : Same as in Fig. 7 for the process
$\bar{p}p \to (D_{\frac{1}{2}} \to q\mu^-\tilde{\chi}) + (\bar{D}_{\frac{1}{2}} \to \bar{q}\mu^+\tilde{\chi}) + x$
a) at $\sqrt{s}$ = 630 GeV and b) at $\sqrt{s}$ = 1600 GeV.

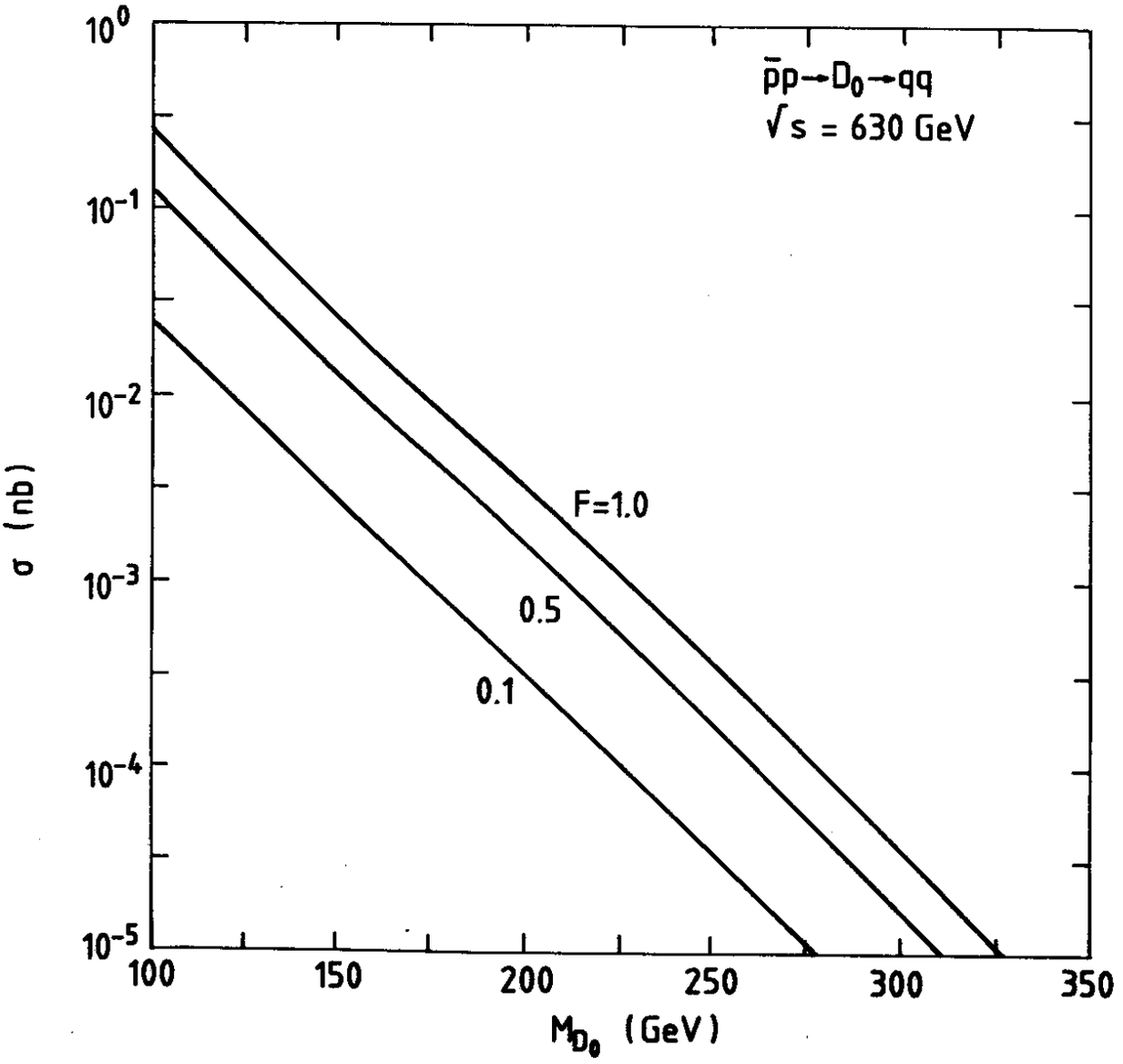
$\bar{p}p \to D_0 \to qq$
$\sqrt{s}$ = 630 GeV
F=1.0
0.5
0.1
σ (nb)
10^0
10^{-1}
10^{-2}
10^{-3}
10^{-4}
10^{-5}
100
150
200
250
300
350
M_{D_0} (GeV)

Fig. 1a

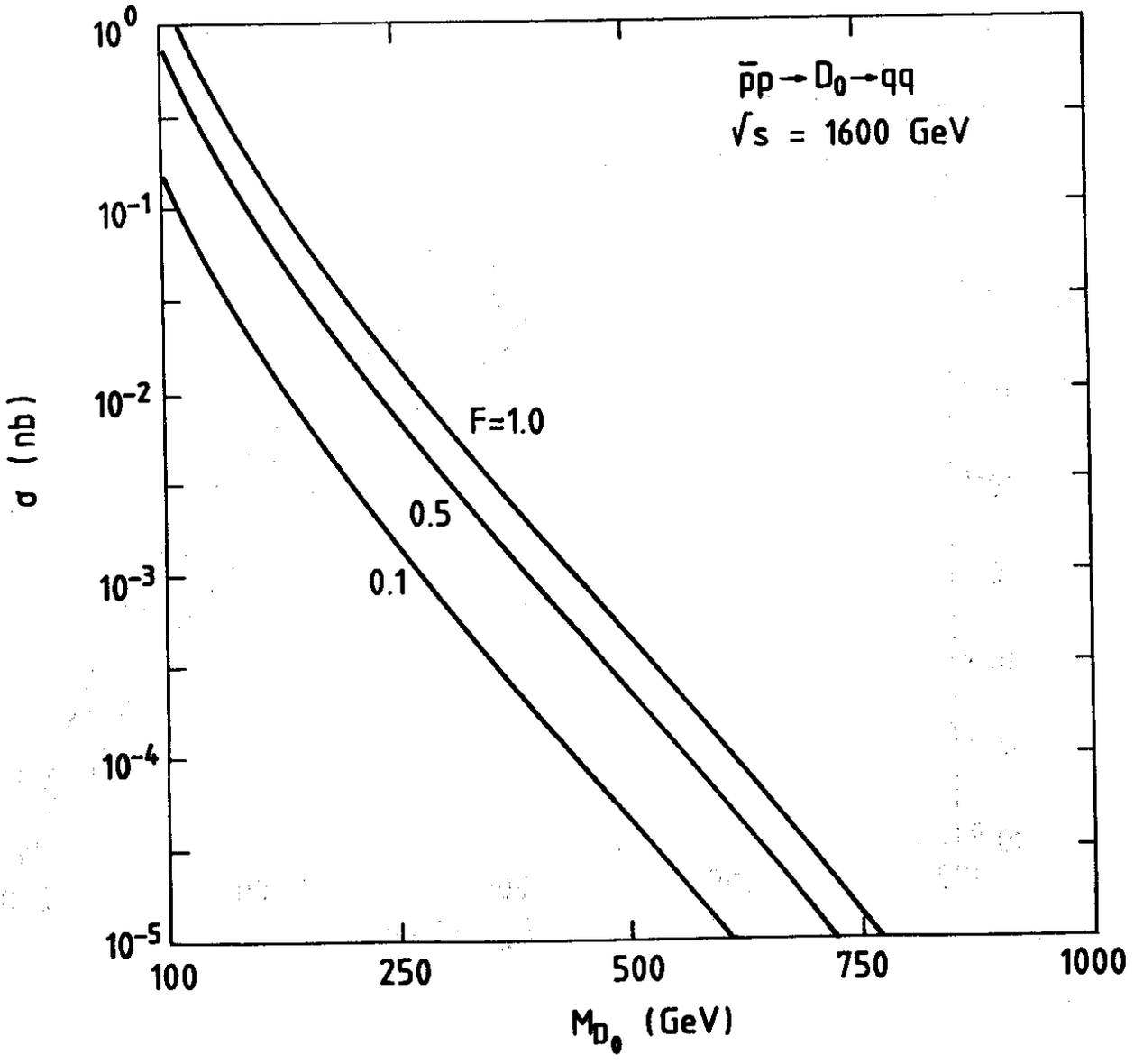
$\bar{p}p \to D_0 \to qq$
$\sqrt{s}$ = 1600 GeV
F=1.0
0.5
0.1
σ (nb)
10^0
10^{-1}
10^{-2}
10^{-3}
10^{-4}
10^{-5}
100
250
500
750
1000
M_{D_0} (GeV)

Fig. 1b

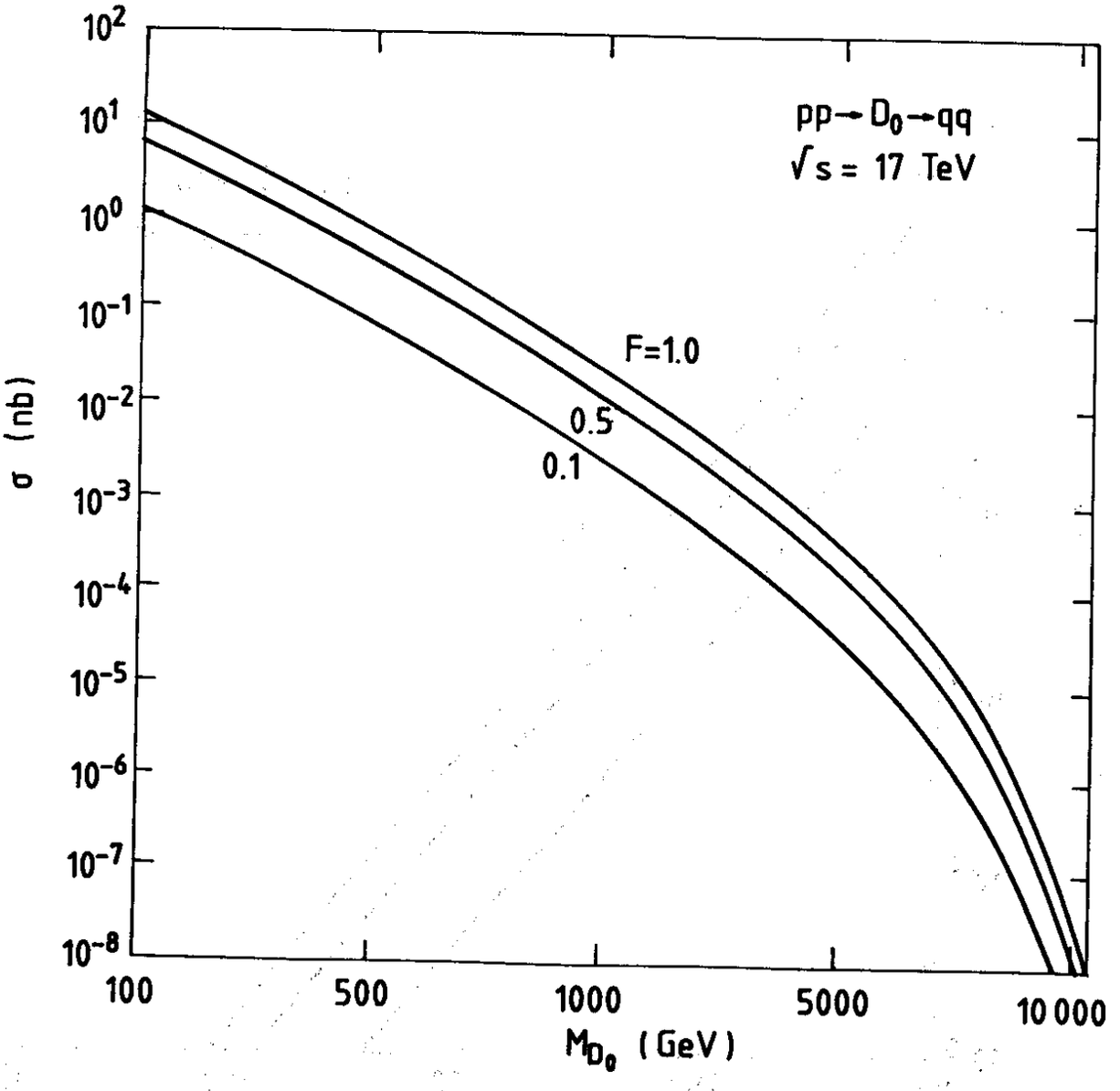
10^2
10^1
10^0
10^{-1}
10^{-2}
10^{-3}
10^{-4}
10^{-5}
10^{-6}
10^{-7}
10^{-8}
σ (nb)
$pp \rightarrow D_0 \rightarrow qq$
$\sqrt{s}$ = 17 TeV
F=1.0
0.5
0.1
100
500
1000
5000
10 000
M_{D_0} (GeV)

Fig. 1c

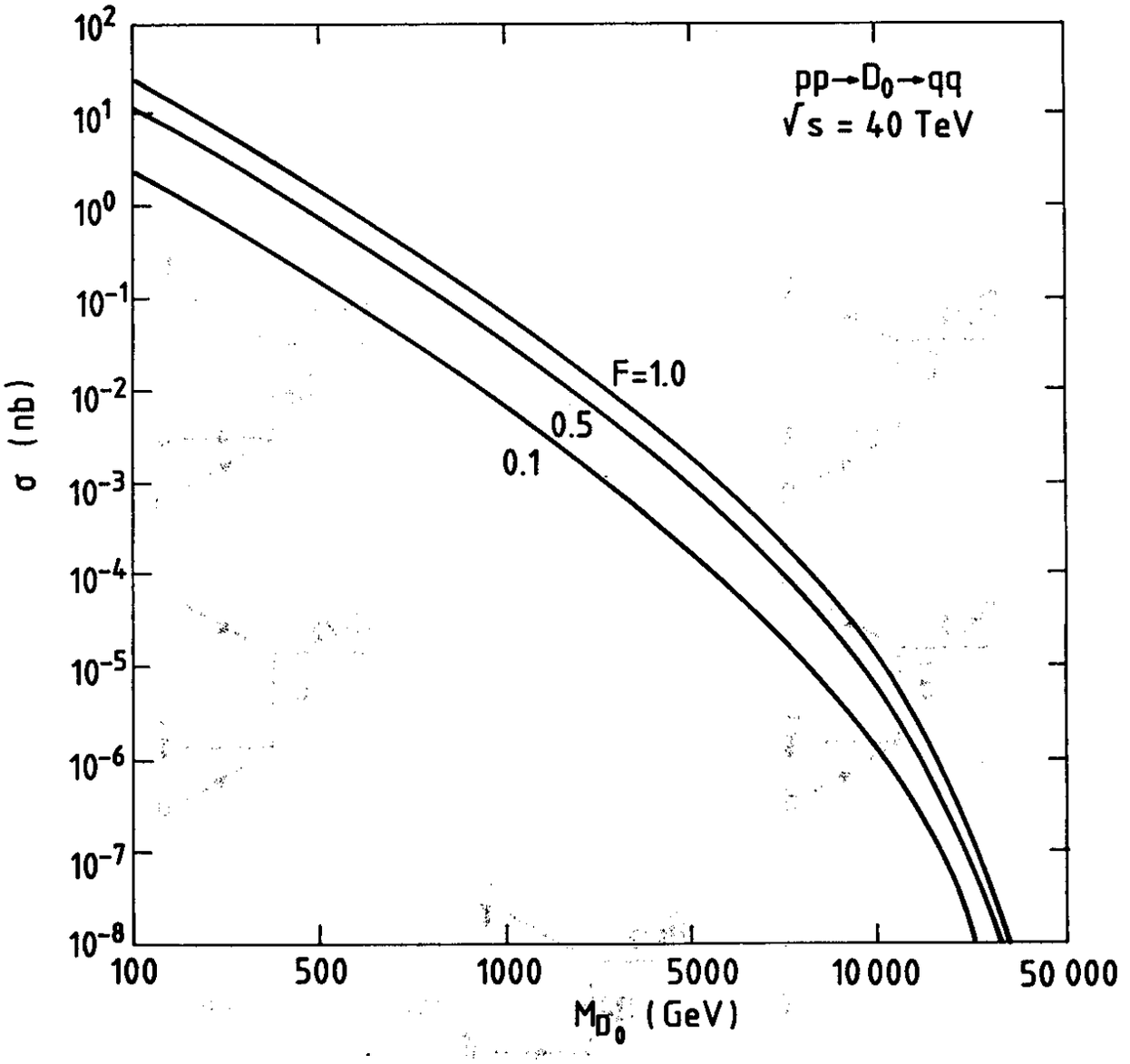
pp→D0→qq
√s = 40 TeV
F=1.0
0.5
0.1
σ (nb)
10^2
10^1
10^0
10^-1
10^-2
10^-3
10^-4
10^-5
10^-6
10^-7
10^-8
100
500
1000
5000
10 000
50 000
M_D0 (GeV)

Fig. 1d

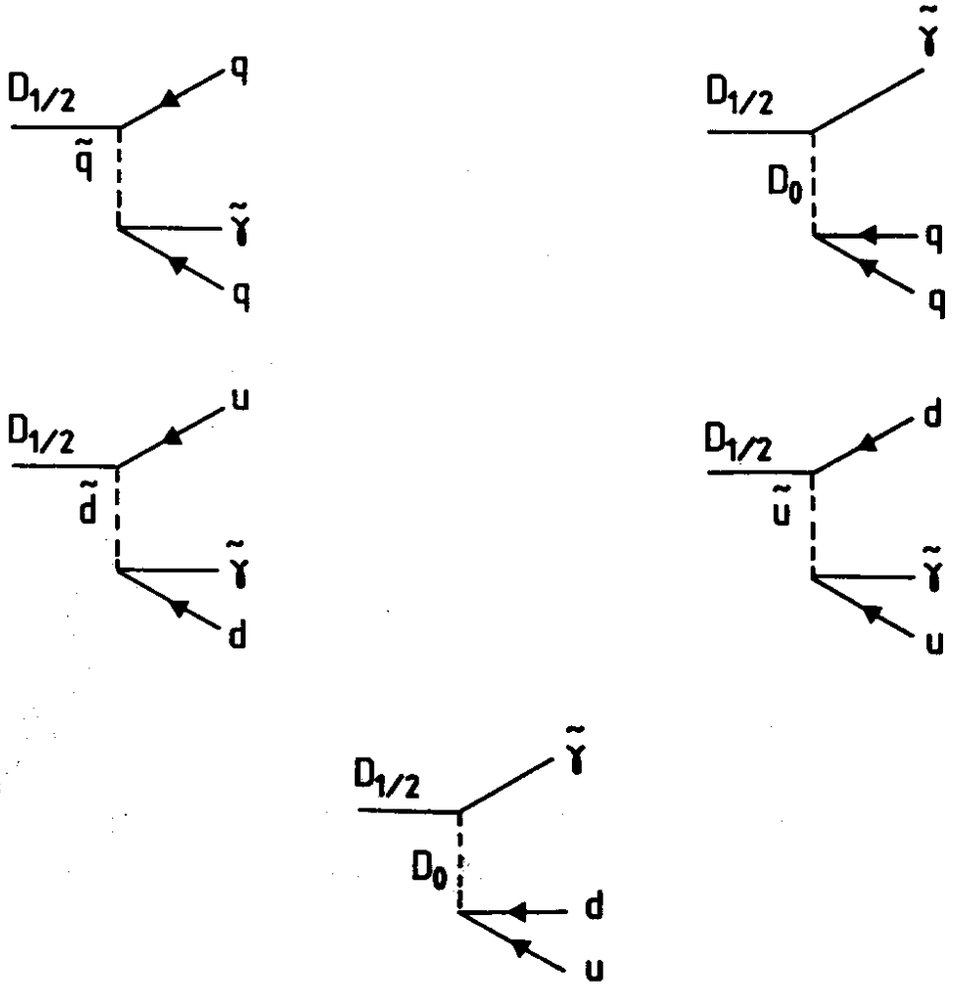
$D_{1/2}$
q
$\tilde{q}$
$\tilde{\gamma}$
q
$D_{1/2}$
$\tilde{\gamma}$
D_0
q
q
$D_{1/2}$
u
$\tilde{d}$
$\tilde{\gamma}$
d
$D_{1/2}$
d
$\tilde{u}$
$\tilde{\gamma}$
u
$D_{1/2}$
$\tilde{\gamma}$
D_0
d
u

Fig. 2

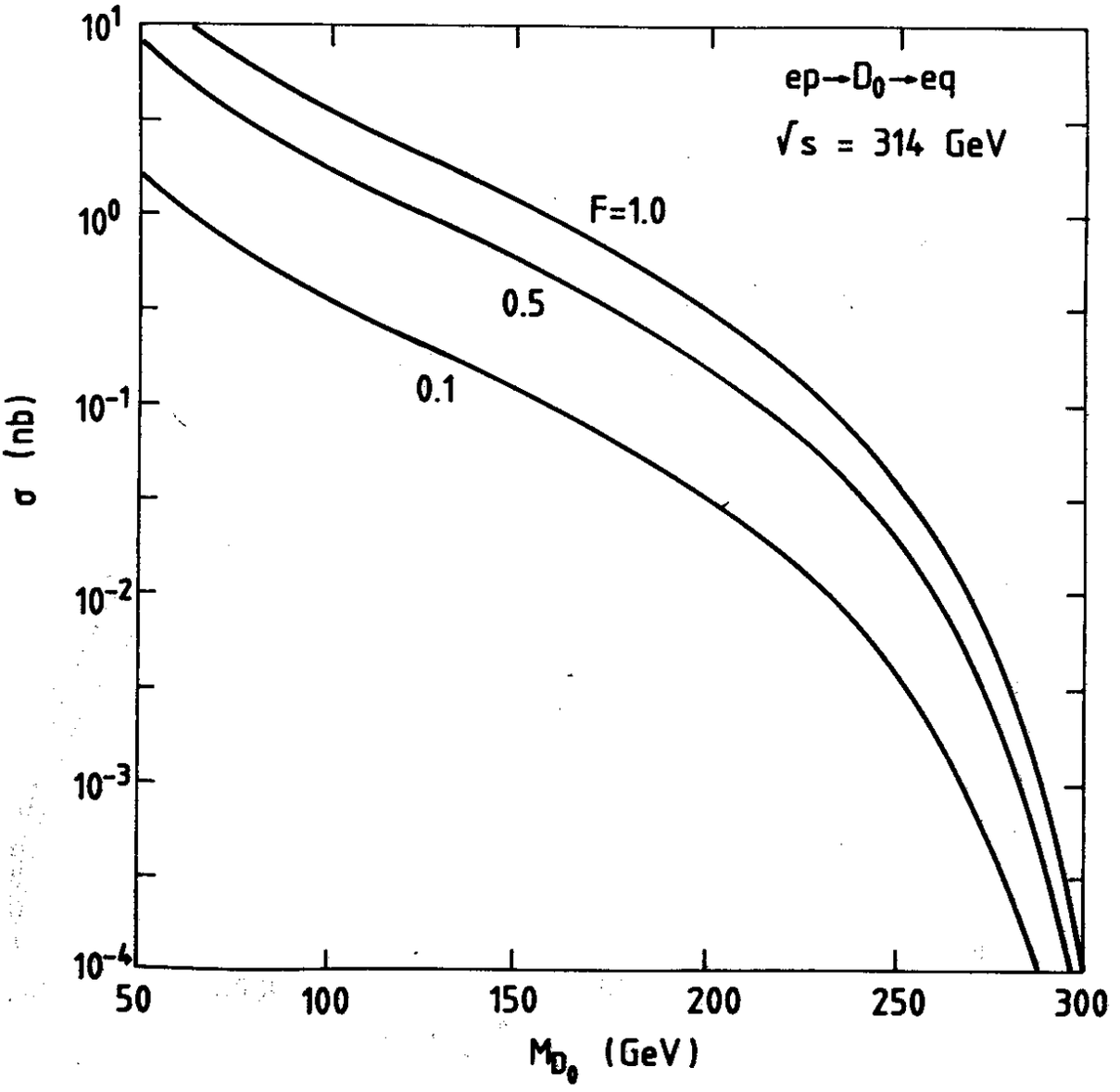
ep→D0→eq
√s = 314 GeV
F=1.0
0.5
0.1
σ (nb)
10^1
10^0
10^-1
10^-2
10^-3
10^-4
50
100
150
200
250
300
M_D0 (GeV)

Fig. 3a

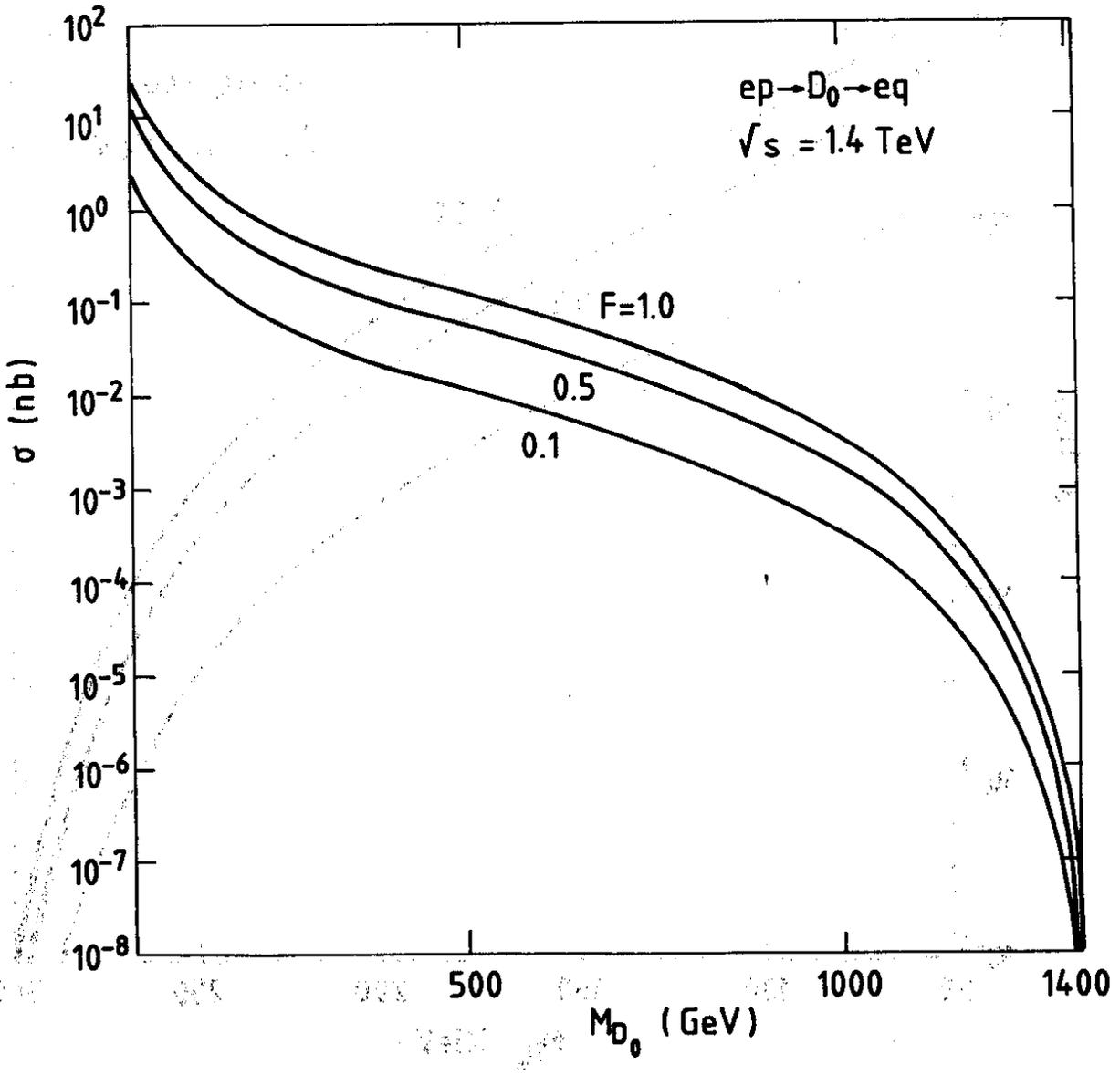
10^2
10^1
10^0
10^{-1}
10^{-2}
10^{-3}
10^{-4}
10^{-5}
10^{-6}
10^{-7}
10^{-8}
σ (nb)
ep→D0→eq
√s = 1.4 TeV
F=1.0
0.5
0.1
500
1000
1400
MD0 (GeV)

Fig. 3b

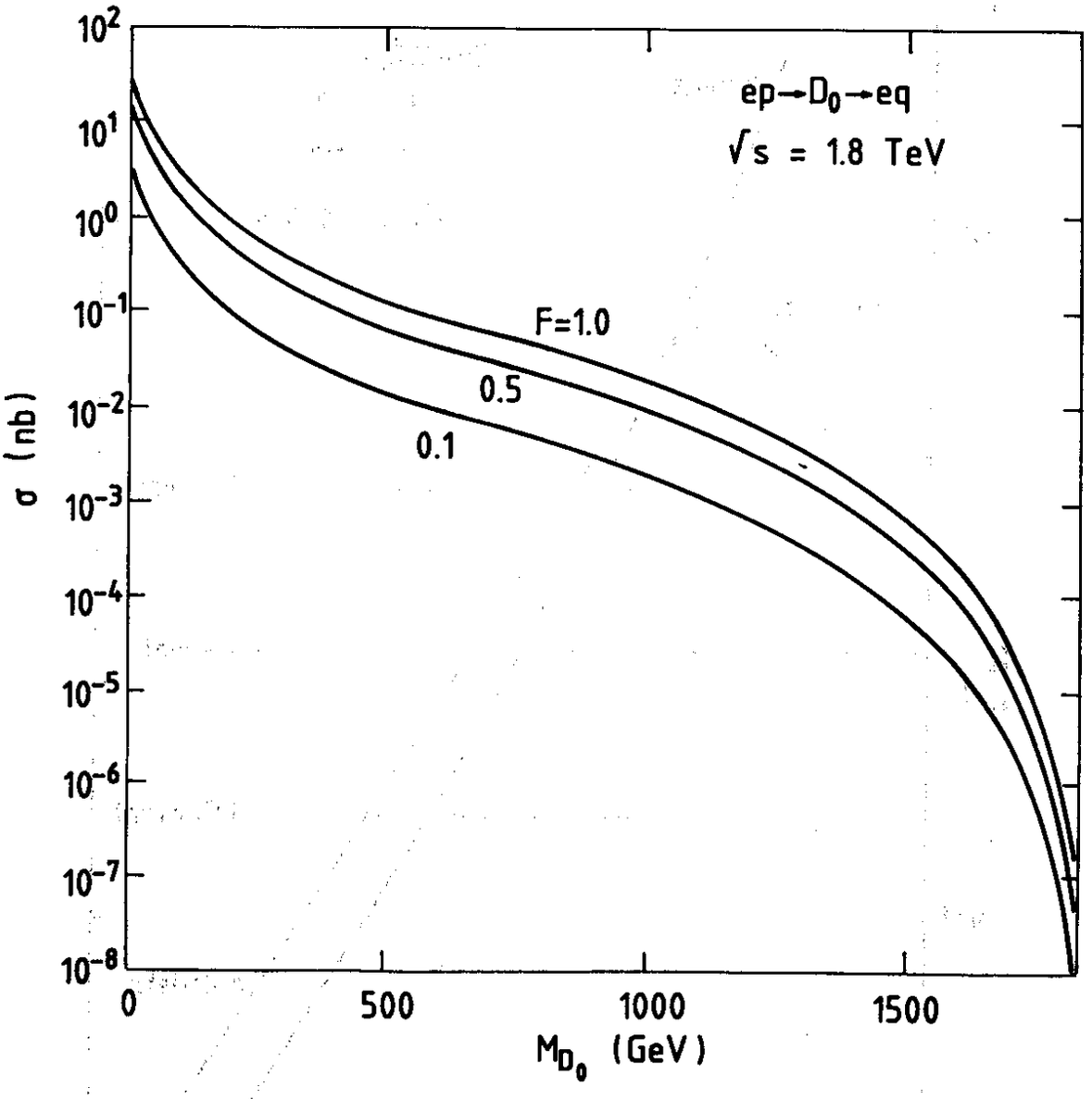
ep→D0→eq
√s = 1.8 TeV
F=1.0
0.5
0.1
σ (nb)
MD0 (GeV)
10^2
10^1
10^0
10^-1
10^-2
10^-3
10^-4
10^-5
10^-6
10^-7
10^-8
0
500
1000
1500

Fig. 3c

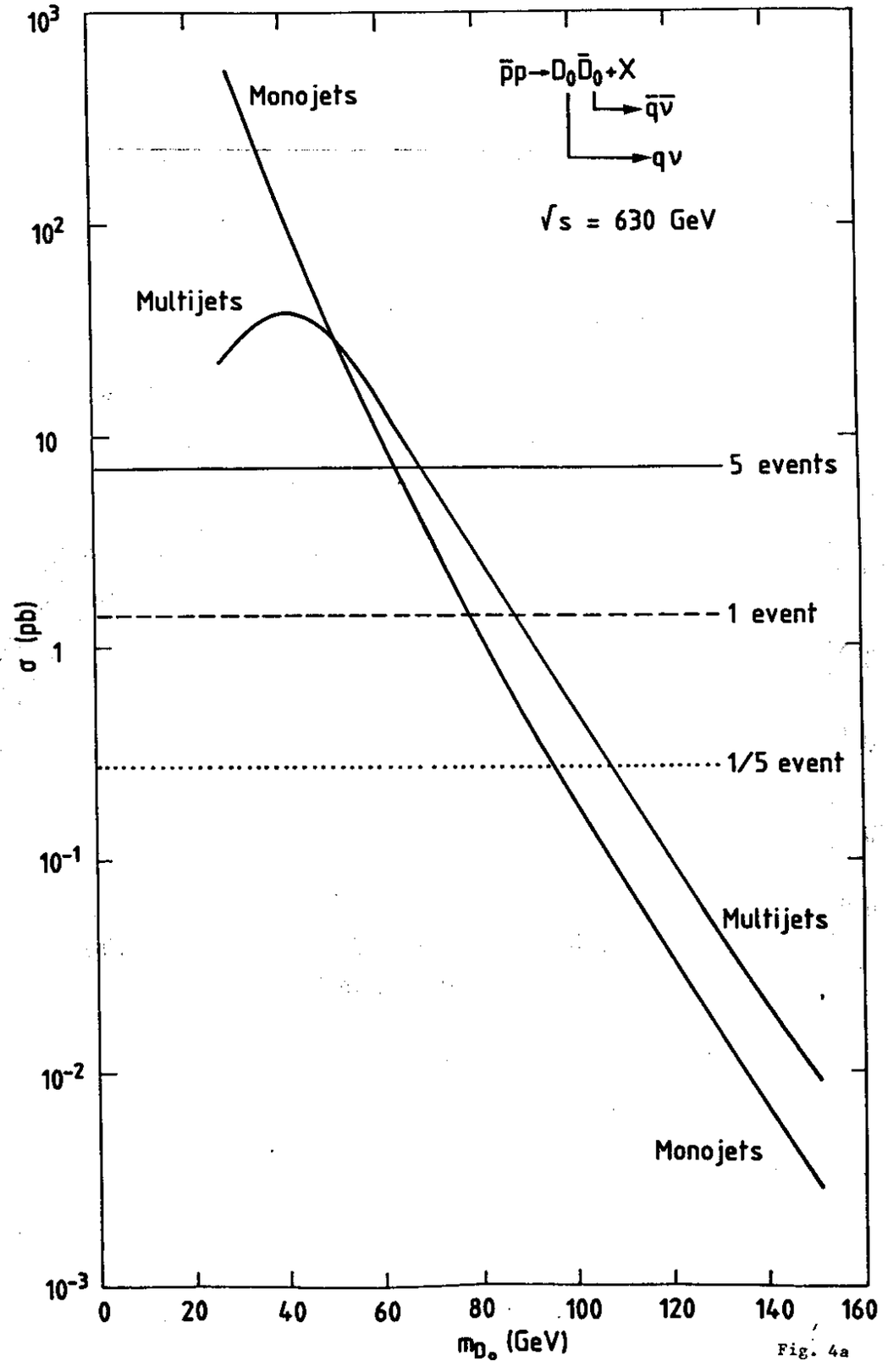
10^3
10^2
10
1
10^{-1}
10^{-2}
10^{-3}
σ (pb)
$\bar{p}p \to D_0\bar{D}_0 + X$
$\bar{q}\nu$
$q\nu$
$\sqrt{s}$ = 630 GeV
Monojets
Multijets
5 events
1 event
1/5 event
Multijets
Monojets
0
20
40
60
80
100
120
140
160
m_{D_0} (GeV)

Fig. 4a

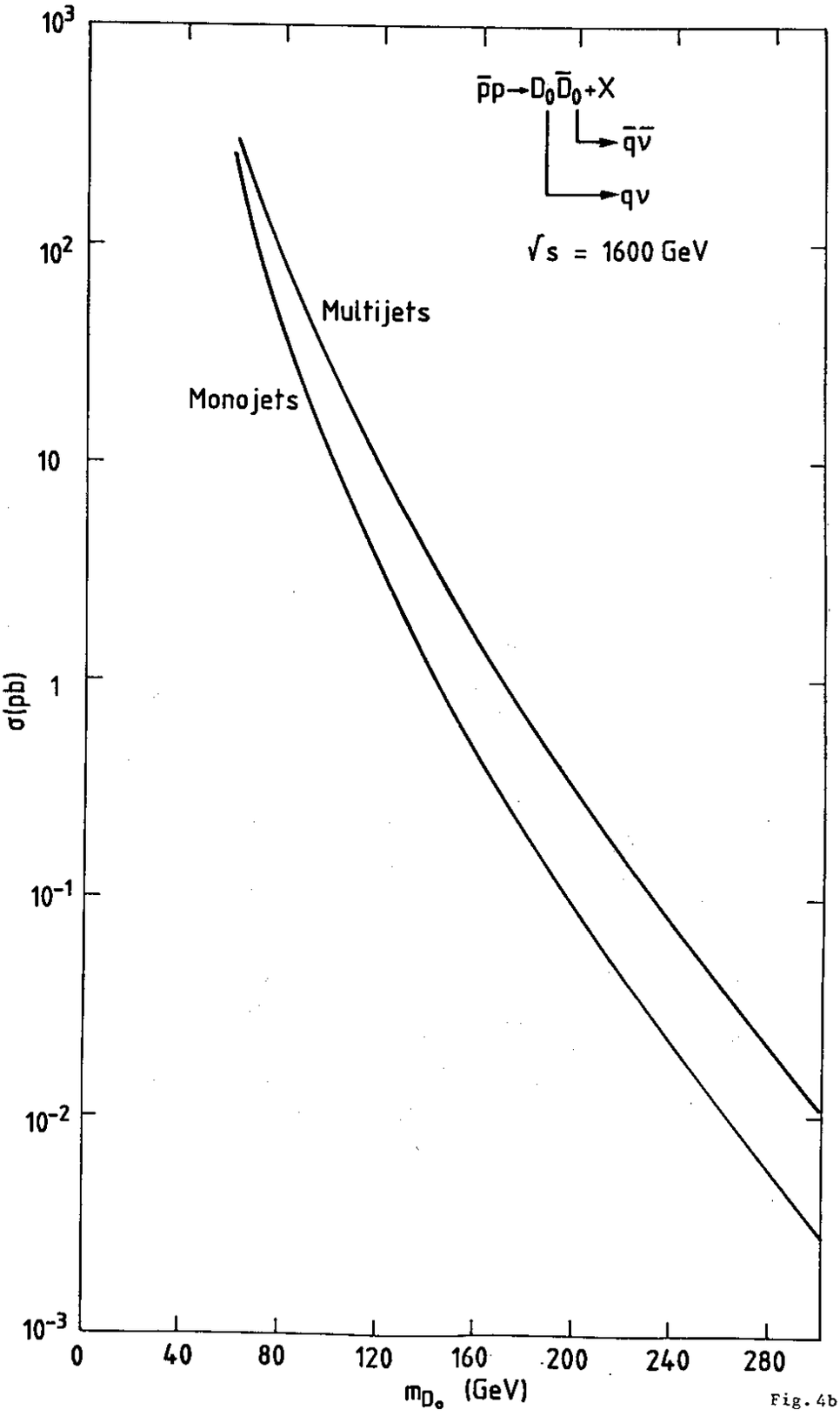
10^3
10^2
10
1
10^{-1}
10^{-2}
10^{-3}
σ(pb)
$\bar{p}p \to D_0\bar{D}_0 + X$
$\bar{q}\bar{\nu}$
$q\nu$
$\sqrt{s}$ = 1600 GeV
Multijets
Monojets
0
40
80
120
160
200
240
280
m_{D_0} (GeV)

Fig. 4b

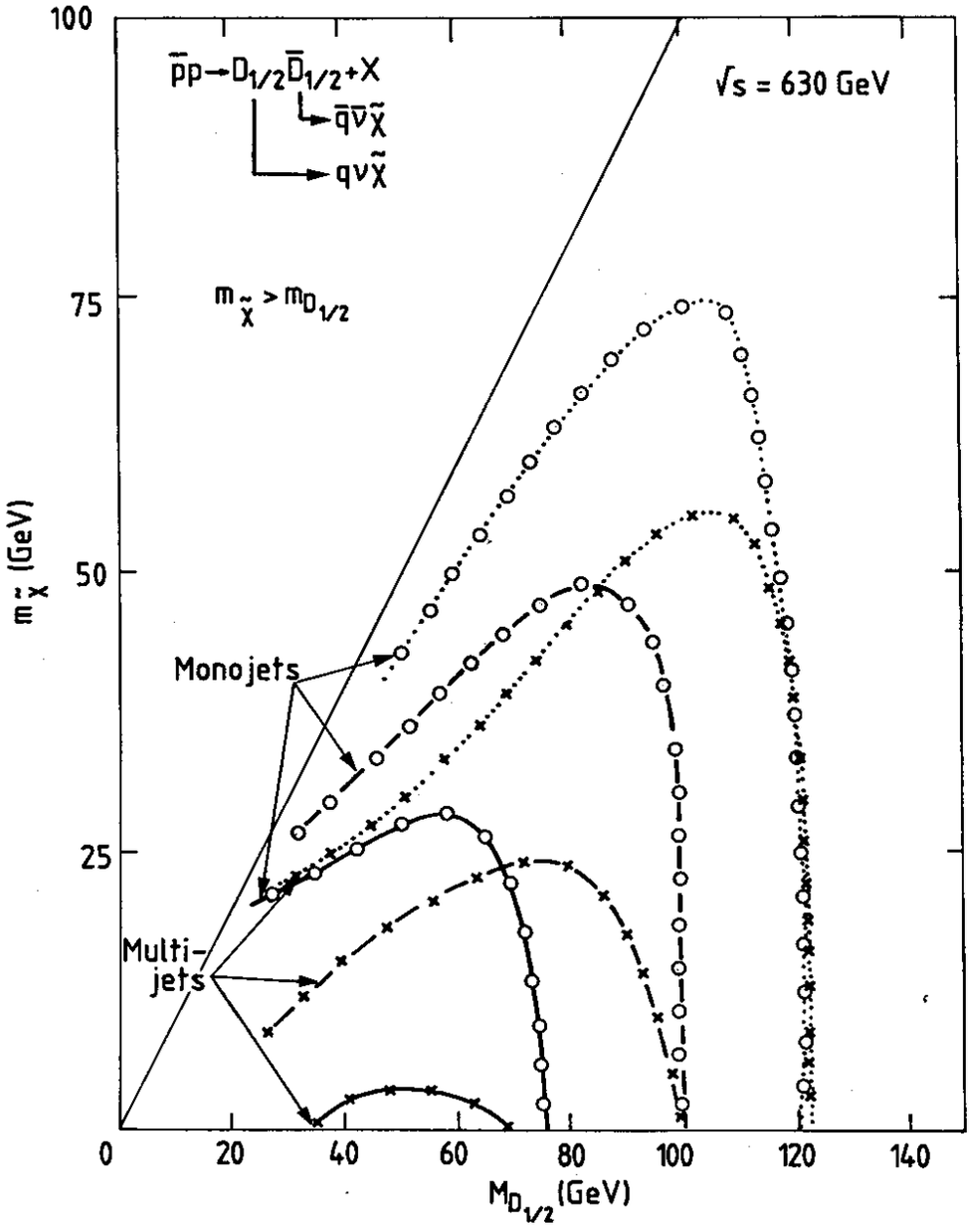
$\bar{p}p \to D_{1/2}\bar{D}_{1/2}+X$
$\bar{q}\nu\tilde{\chi}$
$q\nu\tilde{\chi}$
$\sqrt{s}$ = 630 GeV
$m_{\tilde{\chi}} > m_{D_{1/2}}$
Monojets
Multi-jets
$m_{\tilde{\chi}}$ (GeV)
$M_{D_{1/2}}$ (GeV)
100
75
50
25
0
20
40
60
80
100
120
140

Fig. 5a

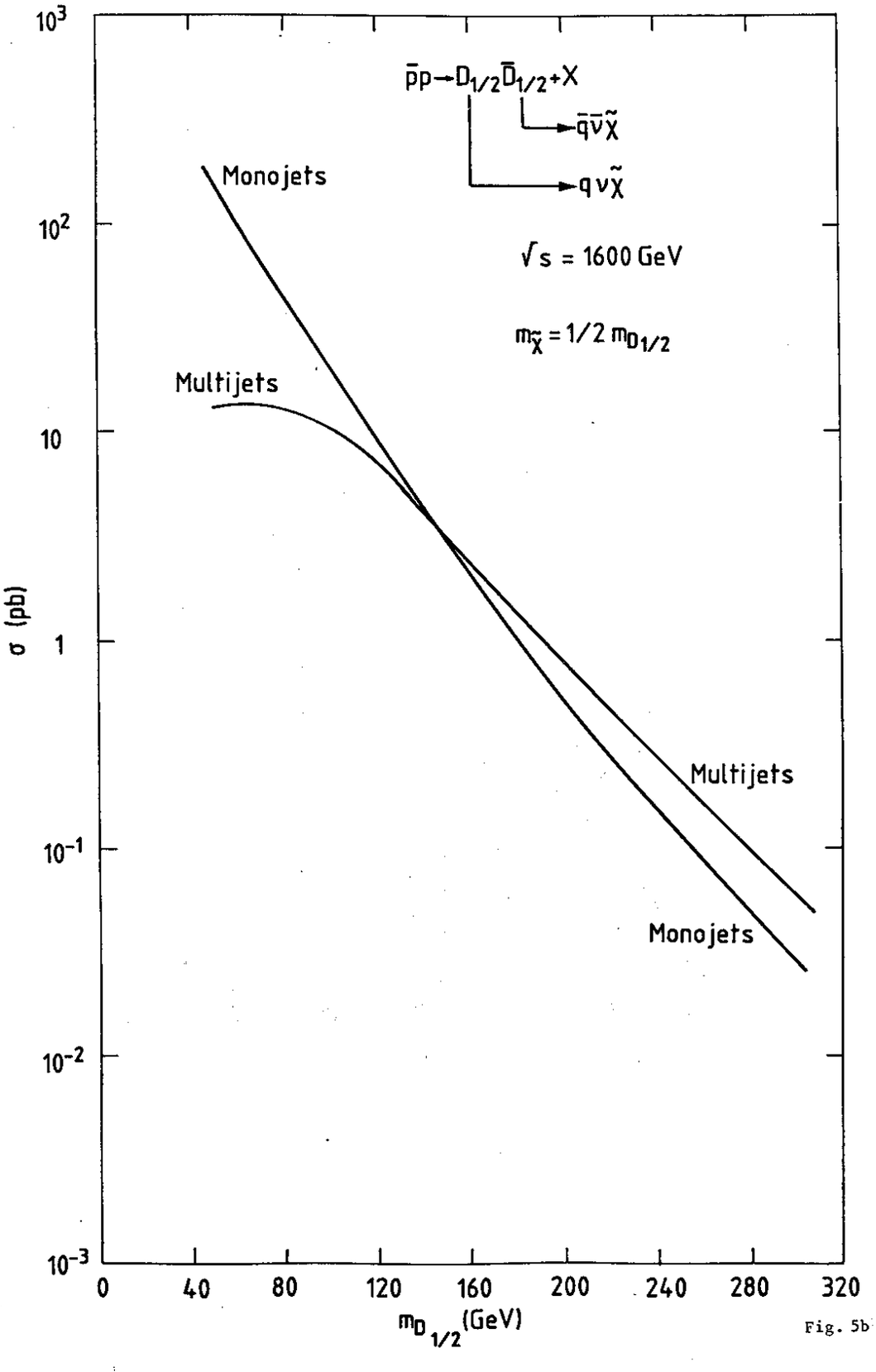
10^3
10^2
10
1
10^{-1}
10^{-2}
10^{-3}
σ (pb)
$\bar{p}p \to D_{1/2}\bar{D}_{1/2}+X$
$\bar{q}\bar{\nu}\tilde{\chi}$
$q\nu\tilde{\chi}$
Monojets
$\sqrt{s}$ = 1600 GeV
$m_{\tilde{\chi}} = 1/2\, m_{D_{1/2}}$
Multijets
Multijets
Monojets
0
40
80
120
160
200
240
280
320
$m_{D_{1/2}}$ (GeV)

Fig. 5b

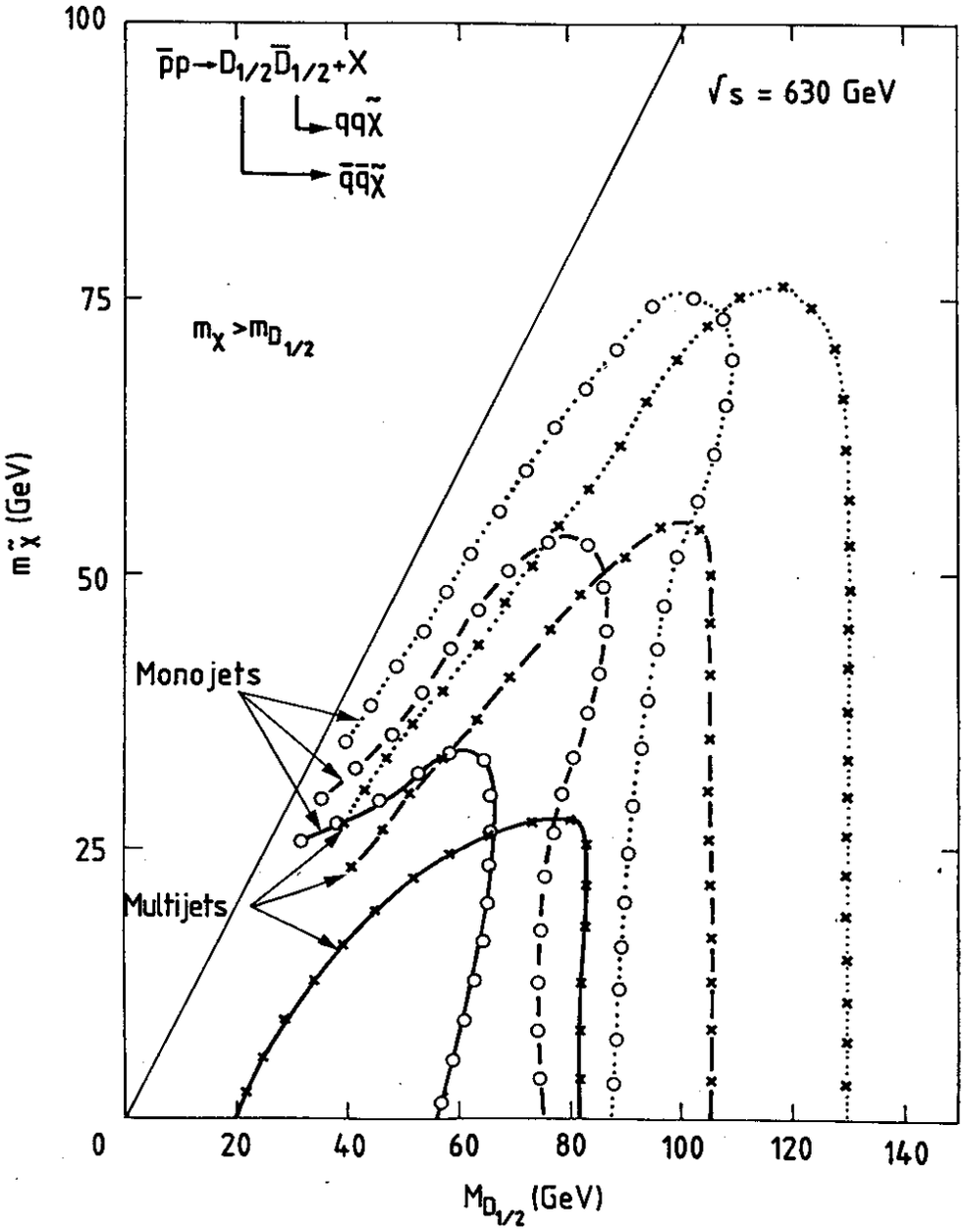
$\bar{p}p \to D_{1/2}\bar{D}_{1/2}+X$
$\hookrightarrow q\bar{q}\tilde{\chi}$
$\hookrightarrow \bar{q}\bar{q}\tilde{\chi}$
$\sqrt{s}$ = 630 GeV
$m_{\chi} > m_{D_{1/2}}$
Monojets
Multijets
$m_{\tilde{\chi}}$ (GeV)
$M_{D_{1/2}}$ (GeV)
0
25
50
75
100
20
40
60
80
100
120
140

Fig. 6a

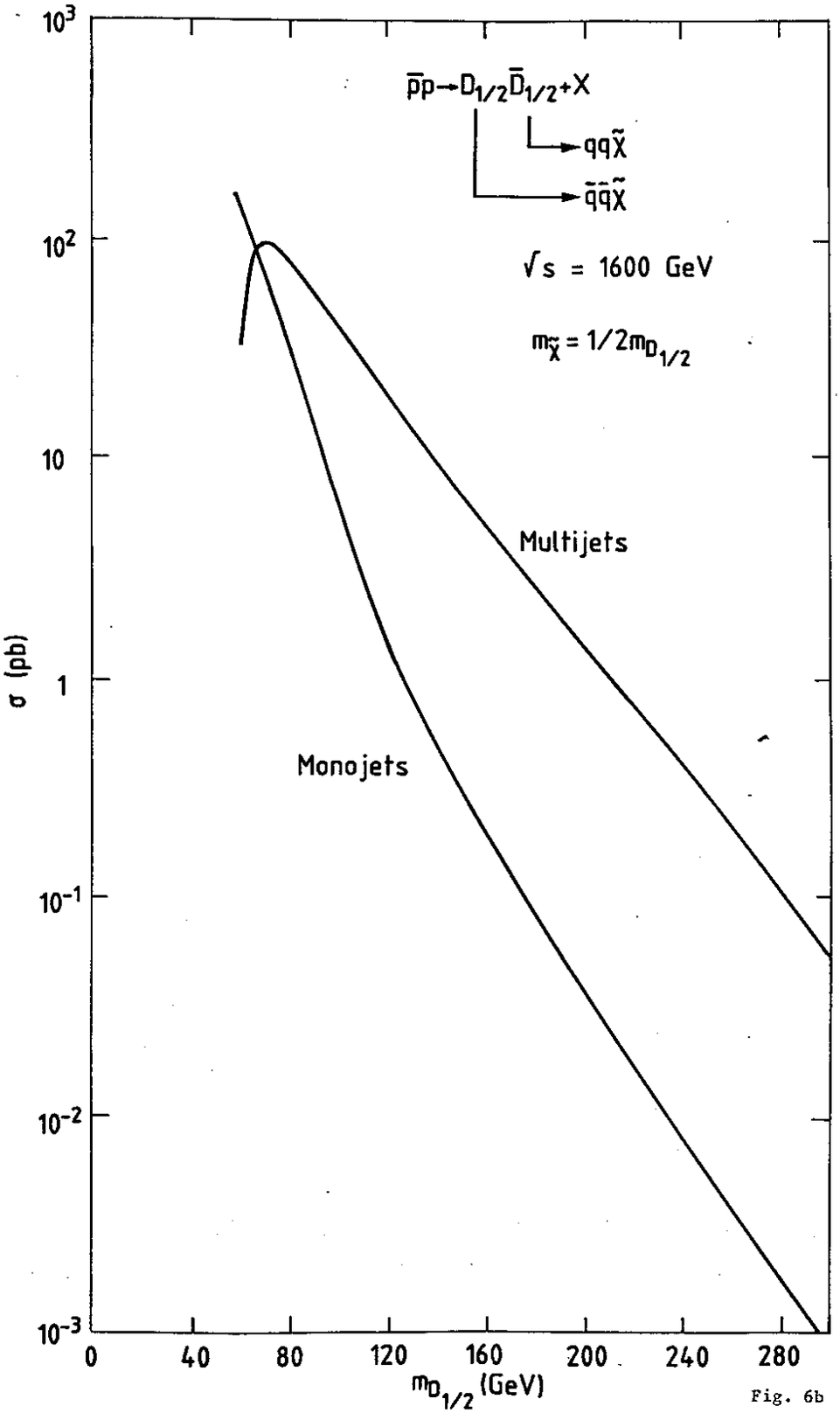
10^3
10^2
10
1
10^{-1}
10^{-2}
10^{-3}
σ (pb)
$\bar{p}p \to D_{1/2}\bar{D}_{1/2}+X$
$\to q\bar{q}\tilde{X}$
$\to \bar{q}\bar{q}\tilde{X}$
$\sqrt{s}$ = 1600 GeV
$m_{\tilde{X}} = 1/2 m_{D_{1/2}}$
Multijets
Monojets
0
40
80
120
160
200
240
280
$m_{D_{1/2}}$ (GeV)

Fig. 6b

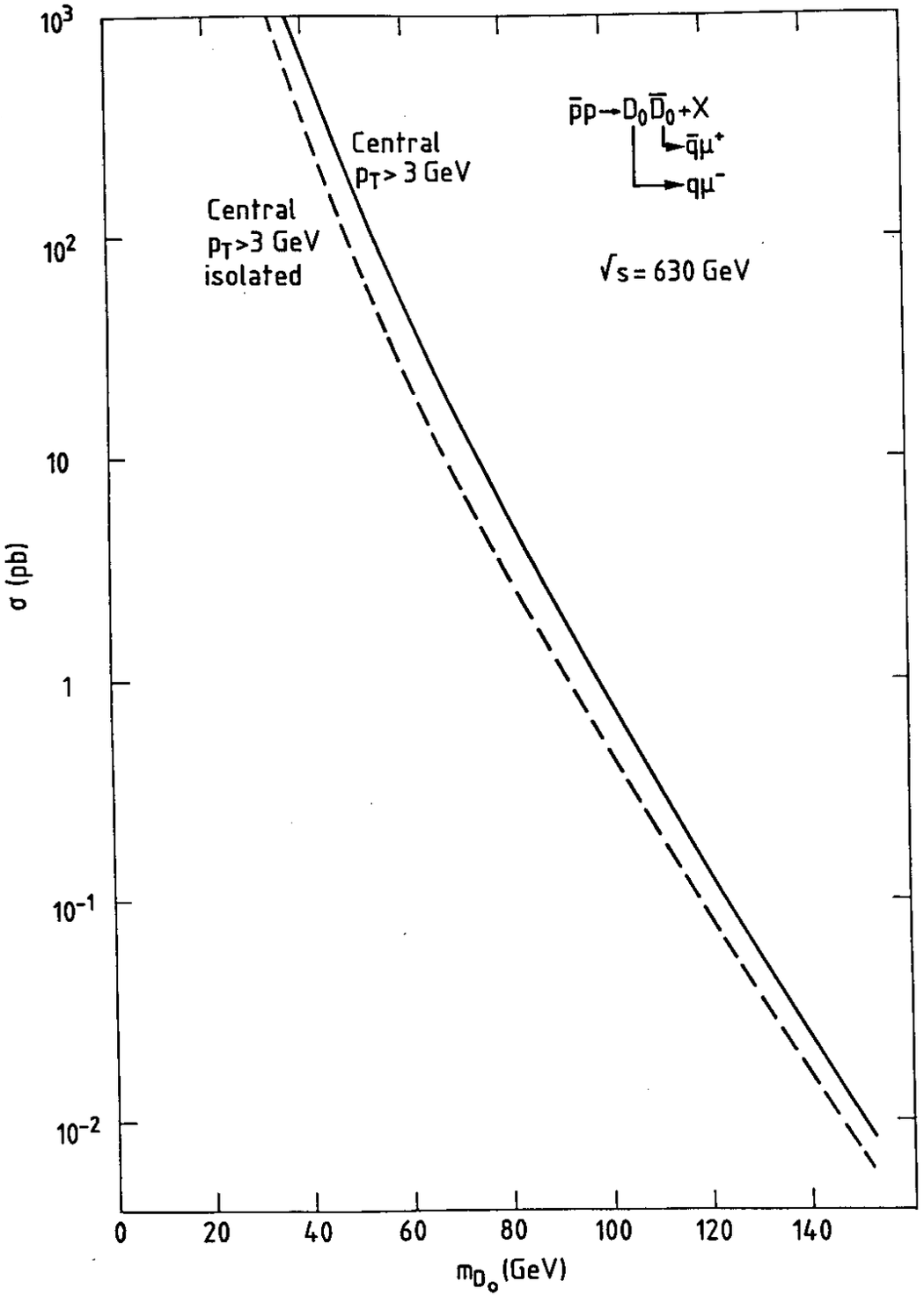
10^3
10^2
10
1
10^{-1}
10^{-2}
σ (pb)
0
20
40
60
80
100
120
140
m_{D_o} (GeV)
$\bar{p}p \to D_0 \bar{D}_0 + X$
$\hookrightarrow \bar{q}\mu^+$
$\hookrightarrow q\mu^-$
Central
$p_T > 3$ GeV
Central
$p_T > 3$ GeV
isolated
$\sqrt{s} = 630$ GeV

Fig. 7a

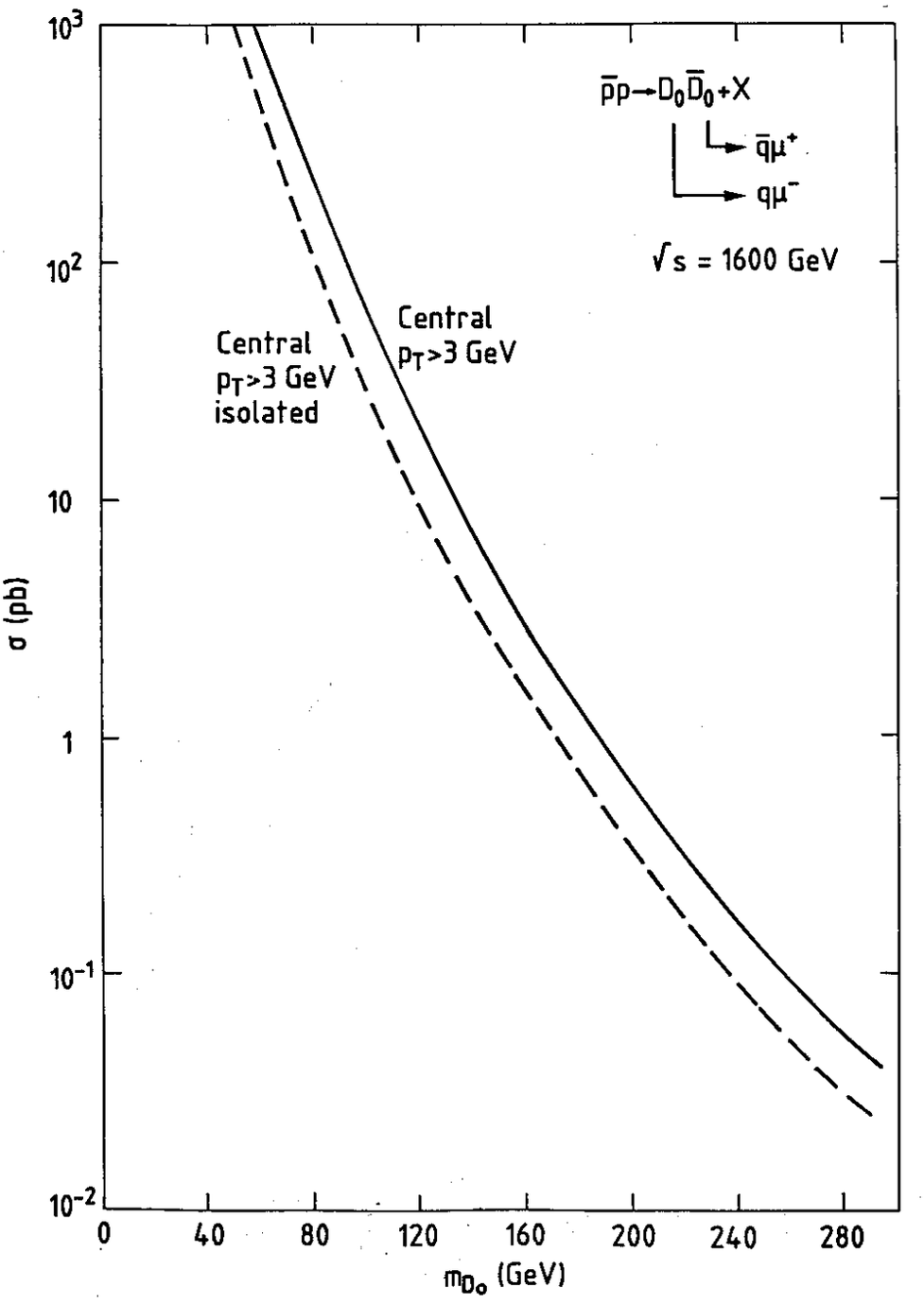
10^3
10^2
10
1
10^{-1}
10^{-2}
σ (pb)
$\bar{p}p \to D_0 \bar{D}_0 + X$
$\bar{q}\mu^+$
$q\mu^-$
$\sqrt{s}$ = 1600 GeV
Central
p_T>3 GeV
Central
p_T>3 GeV
isolated
0
40
80
120
160
200
240
280
m_{D_0} (GeV)

Fig. 7b

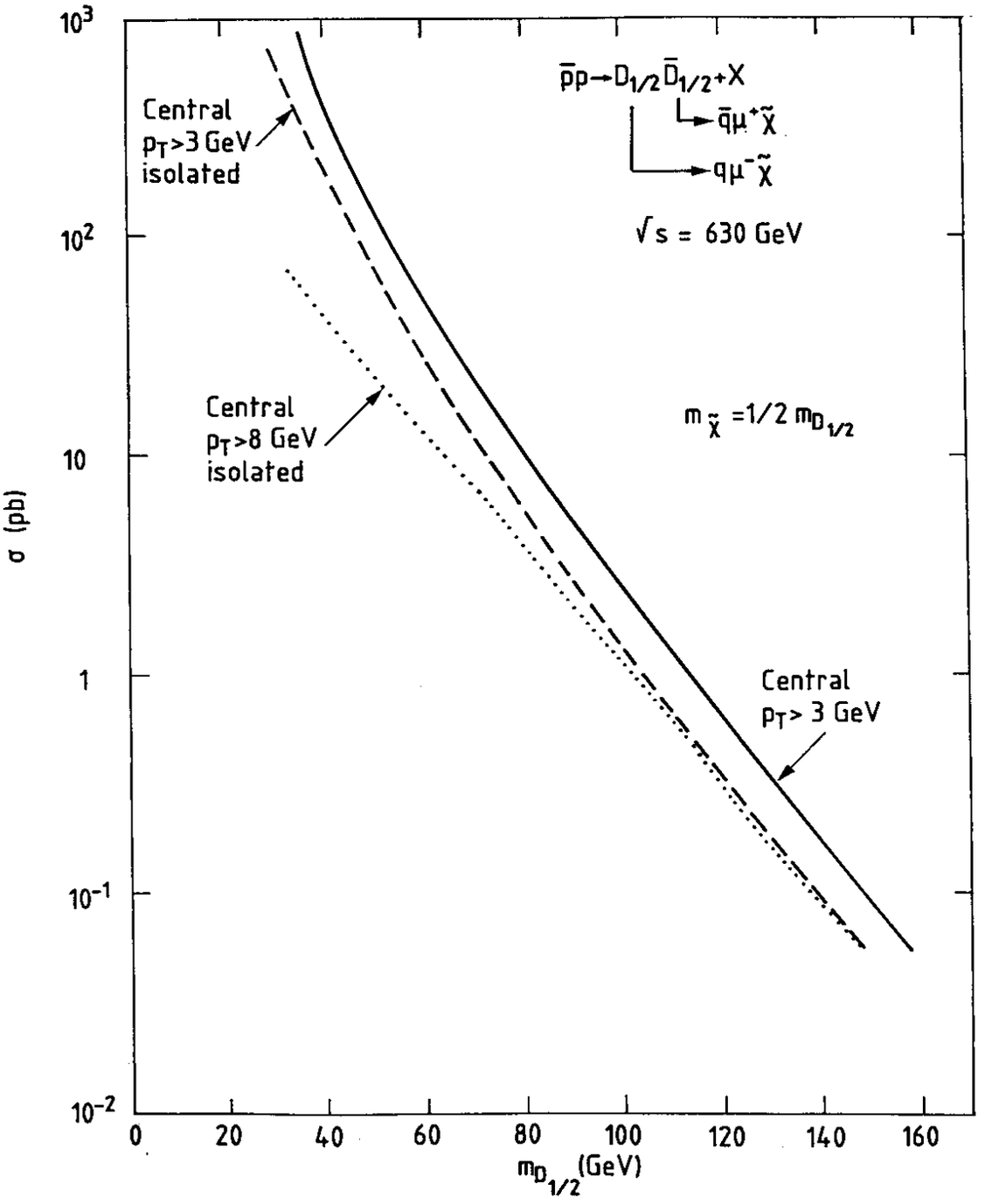
10^3
10^2
10
1
10^{-1}
10^{-2}
σ (pb)
0
20
40
60
80
100
120
140
160
$m_{D_{1/2}}$ (GeV)
$\bar{p}p \to D_{1/2}\bar{D}_{1/2}+X$
$\bar{q}\mu^+\tilde{\chi}$
$q\mu^-\tilde{\chi}$
$\sqrt{s}$ = 630 GeV
$m_{\tilde{\chi}} = 1/2\, m_{D_{1/2}}$
Central
p_T>3 GeV
isolated
Central
p_T>8 GeV
isolated
Central
p_T> 3 GeV

Fig. 8a

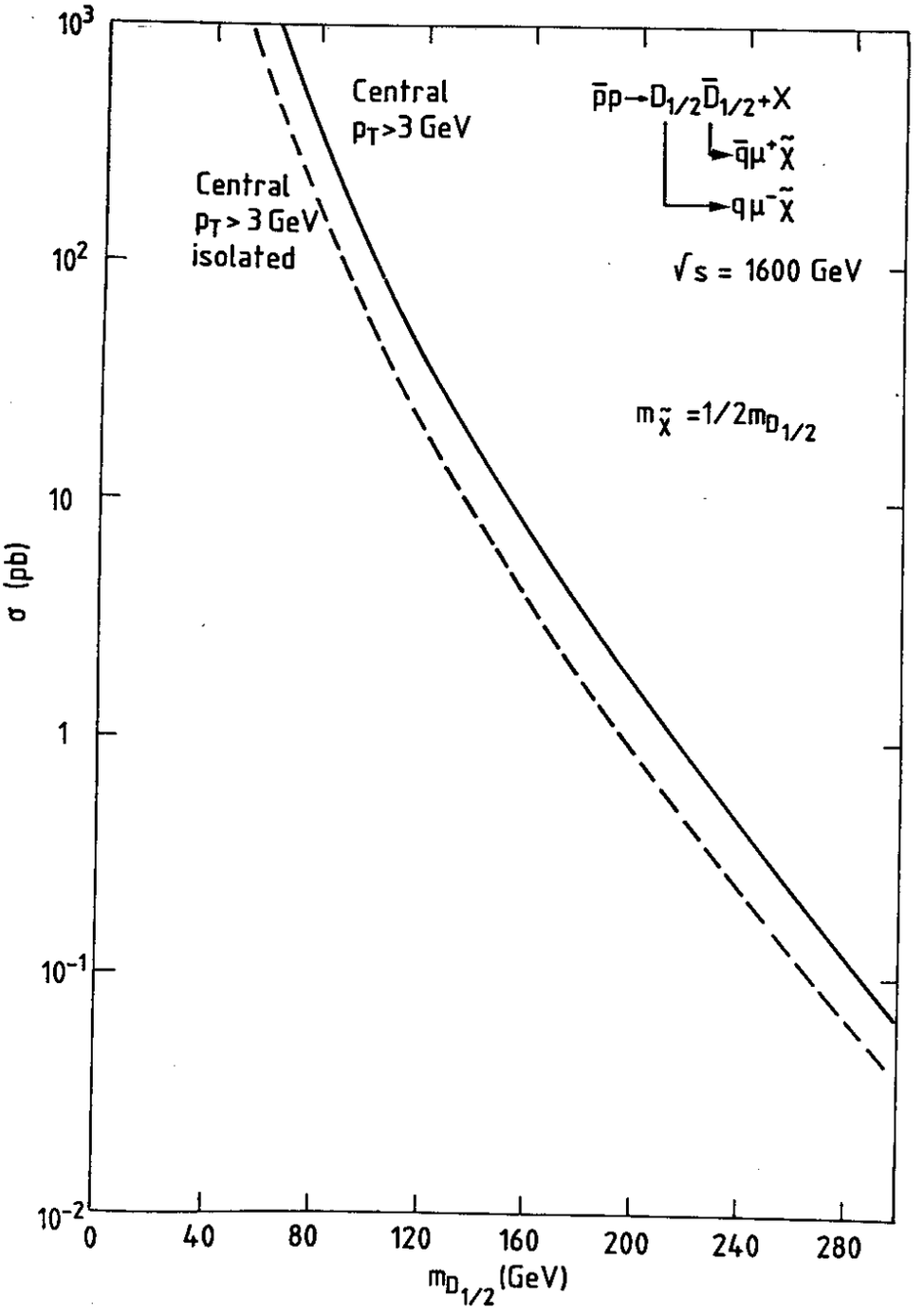
Central
p_T>3 GeV
Central
p_T > 3 GeV
isolated
$\bar{p}p \to D_{1/2}\bar{D}_{1/2}+X$
$\bar{q}\mu^+\tilde{\chi}$
$q\mu^-\tilde{\chi}$
$\sqrt{s}$ = 1600 GeV
$m_{\tilde{\chi}} = 1/2 m_{D_{1/2}}$
10^3
10^2
10
1
10^{-1}
10^{-2}
σ (pb)
0
40
80
120
160
200
240
280
$m_{D_{1/2}}$ (GeV)

Fig. 8b